NBSIR 75-816

PERFORMANCE CHARACTERISTICS OF A LIQUID HELIUM PUMP

P. R. Ludtke

Cryogenics Division
Institute for Basic Standards
National Bureau of Standards
Boulder, Colorado 80302

July 1975

Final Report

Prepared for:
Air Force Aero Propulsion Laboratory
Air Force Systems Command
Wright-Patterson Air Force Base, Ohio 45433

U.S. DEPARTMENT OF COMMERCE, Rogers C. B. Morton, Secretary
John K. Tabor, Under Secretary
Dr. Betsy Ancker-Johnson, Assistant Secretary for Science and Technology

NATIONAL BUREAU OF STANDARDS, Ernest Ambler, Acting Director

SECURITY CLASSIFICATION OF THIS PAGE *(When Data Entered)*

REPORT DOCUMENTATION PAGE

READ INSTRUCTIONS BEFORE COMPLETING FORM

1. REPORT NUMBER: AFAPL-TR-75-40	2. GOVT ACCESSION NO.
3. RECIPIENT'S CATALOG NUMBER	
4. TITLE *(and Subtitle)*: PERFORMANCE CHARACTERISTICS OF A LIQUID HELIUM PUMP.	5. TYPE OF REPORT & PERIOD COVERED: Final Report
6. PERFORMING ORG. REPORT NUMBER: NBSIR-75-816	
7. AUTHOR(s): P. R. Ludtke	8. CONTRACT OR GRANT NUMBER(s): MIPR-FY-14557300411
9. PERFORMING ORGANIZATION NAME AND ADDRESS: Cryogenics Division, Institute for Basic Standards, National Bureau of Standards, Boulder, CO 80302	10. PROGRAM ELEMENT, PROJECT, TASK AREA & WORK UNIT NUMBERS: 62405H45, 3145320[illegible]
11. CONTROLLING OFFICE NAME AND ADDRESS: Air Force Aero Propulsion Laboratory, AFAPL/POD-1, Wright-Patterson AFB, OH 45433	12. REPORT DATE: June 1975
	13. NUMBER OF PAGES: 50
14. MONITORING AGENCY NAME & ADDRESS *(if different from Controlling Office)*	15. SECURITY CLASS. *(of this report)*: Unclassified
	15a. DECLASSIFICATION/DOWNGRADING SCHEDULE

16. DISTRIBUTION STATEMENT *(of this Report)*

Approved for public release; distribution unlimited.

17. DISTRIBUTION STATEMENT *(of the abstract entered in Block 20, if different from Report)*

18. SUPPLEMENTARY NOTES

19. KEY WORDS *(Continue on reverse side if necessary and identify by block number)*

Cavitation; cryogenic motors; induction motors; liquid helium pumps; motor efficiency; net positive suction head; pump efficiency; pump performance.

20. ABSTRACT *(Continue on reverse side if necessary and identify by block number)*

Part A of this report presents performance data for a simple, preinduced, single stage, centrifugal liquid helium pump powered by a close-coupled submersible cryogenic induction motor. Data on pump efficiency and the motor efficiency are given, and the effects of decreasing the pump leakage loss and removing the pre-inducer were also investigated.

Part B describes a study of the cavitation characteristics of the pump in liquid helium I. The net positive suction head at cavitation of the pump was extensively investigated, and found to be near zero; and effects of removing the inducer, changing the pump inlet geometry, and varying the helium temperature were also determined.

DD FORM 1 JAN 73 1473 EDITION OF 1 NOV 65 IS OBSOLETE

Unclassified

SECURITY CLASSIFICATION OF THIS PAGE *(When Data Entered)*

Table of Contents

List of Figures and Tables

Terminology

Capital Letters

A_o = area of the pump inlet at elevation Z_o

H = total dynamic head

LL = helium liquid level above Z_o

N = motor or pump speed

Nsf = speed of the stator field in the electric motor

NPSH = net positive suction head

NPSHc = net positive suction head at cavitation

P_o = static pressure at the pump inlet, elevation = Z_o

P_1 = static pressure at the pressure tap in the helium bath located at elevation Z_1

P_{1g} = gauge pressure from the capillary tubing terminating at Z_1

P_2 = static pressure at the pump discharge pressure tap located at elevation Z_2

P_{2g} = gauge pressure from the capillary tubing terminating at the pump discharge, elevation Z_2

Q = pump capacity

S = induction motor slip = $\frac{Nsf - N}{Nsf} \times 100$

T = temperature, kelvin

V_o = average fluid velocity at the inducer entrance, elevation Z_o

$\frac{V_o^2}{2g}$ = fluid velocity head at the pump entrance

V_1 = average fluid velocity at the static pressure tap, P_1

V_2 = average fluid velocity within the pump discharge tube at the static pressure tap P_2, elevation Z_2

$\frac{V_2^2}{2g}$ = fluid velocity head within the pump discharge tube at the static pressure tap P_2, elevation Z_2

W_f = fluid power

W_{sh} = pump shaft power

Z_o = pump reference datum plane (at inducer leading edge)

Z = elevation above the reference plane Z_o

$Z_2 - Z_1$ = pump elevation head = 7 cm

Lower Case Letters

g = local acceleration of gravity

h_ℓ = pump entry head losses

h_o = absolute static pressure head at the pump inlet (elevation = Z_o)

h_u = head generated by the ullage pressure

h_v = head due to the vapor pressure of the fluid at the pump entrance, at elevation Z_o

$\dot{m}$ = mass rate of flow through the pump

u_t = inducer tip speed

v_v = specific volume of the vapor

v_ℓ = specific volume of the liquid

Greek Symbols

η_h = pump hydraulic efficiency

η_t = total efficiency of the pump and motor

η_m = efficiency of the electric motor

η_v = pump volumetric efficiency

η_p = gross efficiency of the pump

ρ = fluid density

Φ = inducer flow coefficient, V_o/u_t

PERFORMANCE CHARACTERISTICS OF A LIQUID HELIUM PUMP*

P. R. Ludtke

Cryogenics Division
Institute for Basic Standards
National Bureau of Standards
Boulder, Colorado 80302

Abstract

Part A of this report presents performance data for a simple, preinduced, single stage, centrifugal liquid helium pump powered by a close-coupled submersible cryogenic induction motor. Data on pump efficiency and the motor efficiency are given, and the effects of decreasing the pump leakage loss and removing the pre-inducer were also investigated.

Part B describes a study of the cavitation characteristics of the pump in liquid helium I. The net positive suction head at cavitation of the pump was extensively investigated, and found to be near zero; the effects of removing the inducer, changing the pump inlet geometry, and varying the helium temperature were also determined.

Key words: Cavitation; cryogenic motors; induction motors; liquid helium pumps; motor efficiency; net positive suction head; pump efficiency; pump performance.

Introduction

In an earlier report, the design, assembly, and preliminary testing of a small submersible centrifugal helium pump were described [1]. That work showed that the pump performance in liquid nitrogen and in normally boiling, supercritical, and even superfluid helium was consistent with standard scaling laws for predicting pump performance, though the developed head was less than that specified by design. In the limited time available for testing, only the combined efficiency of the pump and motor was measured, but not the efficiency of the pump itself; also, some preliminary evidence of cavitation in boiling liquid was given.

This report presents further studies on the same pump. It is divided into two parts, (A) evaluation of pump efficiency, and improvements in pump performance suggested by both the earlier work and the current laboratory tests, and (B) an attempt to study the cavitation characteristics using correlative techniques which have been developed in our laboratory [2] for other cryogenic fluids.

A number of tests were conducted with the small liquid helium pump. The purposes of the tests were:

Part A

1) to compare the previous pump performance data with the new test data taken after making improvements to the pump, and
2) to plug the motor coolant holes in the pump and determine if this improves the pump performance characteristics, and
3) to measure the induction motor efficiency at various operating conditions in liquid helium and liquid nitrogen, and
4) to calculate the pump efficiency at different operating conditions using the motor efficiency and total efficiency values, and

Part B

1) to conduct a thorough investigation of the cavitation characteristics of the helium pump, and
2) to use the cavitation data obtained to check two different cavitation models (generated from LH_2 cavitation data) and determine if the computer models can be used to predict cavitation characteristics for different fluids (He) and pumps of different geometries.

*Studies reported as Part (A) of this report were funded by the Wright-Patterson Air Force Base, and studies reported as Part (B) were funded by the Defense Advanced Research Projects Agency.

A. Pump Performance and Efficiency

A.1 Measurement of the Electric Motor Efficiency

The helium pump and the induction motor are rigidly connected together, and the total efficiency of both units can be easily determined by measuring net electrical power into the motor and fluid power out of the pump. It was decided that in our case the most straightforward method of determining the pump efficiency is to measure the efficiency of the motor separately as a function of shaft speed and input power and frequency, and then calculate the efficiency of the pump using the motor efficiency and the measured total efficiency.

The motor originally powered a small circulating fan in liquid oxygen vessels to inhibit thermal stratification. The motor is an 8-pole induction type, designed for 3-phase 400 Hz input power, with a maximum power rating of 35 watts. At 400 Hz the stator field rotation speed is 6000 rpm†. The circulating fan was removed and replaced by an agitator in order to measure the efficiency of the motor.

A.1.1. Description of the Motor Efficiency Test Apparatus

A special experimental apparatus was designed and built to measure the motor efficiency in liquid helium. A cross-section of the apparatus is shown in figure 1, and photos of the apparatus are shown in figures 2, 3, and 4. The induction motor is clamped into a movable yoke which is suspended by a stainless steel torque rod from the top plate. The motor and yoke assembly is thus free to rotate ± 15 degrees from a neutral position. There is a stationary baffle plate below the yoke and motor assembly that serves to center the motor and inhibit swirling of the helium during a test. Three additional baffle plates were attached to the stationary rods around the periphery of the motor. This was necessary because liquid helium swirling around the motor could exert drag on the motor body which would tend to decrease the torque reading from the motor. A ball bearing centers the motor shaft in the baffle plate. Agitators of three different sizes were used to load the motor in order to measure the efficiency under different loading conditions.

A thick disc of high density polystyrene foam prevents circulation of the cold helium gas on the underside of the top plate. The liquid helium fill line and the vent gas line pass through stainless steel standoff tubes attached to the top plate. This allows the brass top plate to remain near ambient temperature during tests. The 3-phase power and motor speed sensor wires are attached to the motor yoke, extending up through the foam and out through an ambient temperature rubber seal on the top plate.

The entire assembly is placed inside of, and is supported by a 15 cm diameter glass dewar. This dewar is then placed inside a larger glass dewar filled with liquid nitrogen for thermal shielding. The motor and yoke assembly is supported by the ambient temperature bearing in the top plate. The bottom bearing carries no thrust, and any frictional drag from this bearing introduces no error in the torque measurements, since it merely exerts additional drag on the motor.

A torque transducer is firmly attached to the assembly above the brass top plate. Flexible helical connectors were used on each side of the transducer to compensate for any misalignment. The transducer senses the torque on the motor body which is equal and opposite to the torque on the motor shaft, and a calibrated meter provides a visual indication of the torque value.

A 3-phase power supply having variable voltage (0-150 V line-neutral) and variable frequency (50-3600 Hz) was used to power the motor. A polyphase wattmeter was used to measure the electrical power into the motor; a small correction was necessary for power consumed by the wattmeter. A counter was used to sense the motor speed. Values for the motor speed and torque were then used to calculate the power output of the motor.

A.1.2. Motor Efficiency Test Procedure

Each of the glass dewars was purged with either nitrogen or helium gas. A thorough purge of the inner vessel was necessary to insure that all moisture was removed from the

† In order to present the pump performance data concisely and in the terminology widely accepted in the pump field, the pump and motor speed is given in units of revolutions per minute (rpm) in the text. The SI units of radians/second (rad/s) are given on all the pump performance graphs, along with the conventional units of revolutions per minute.

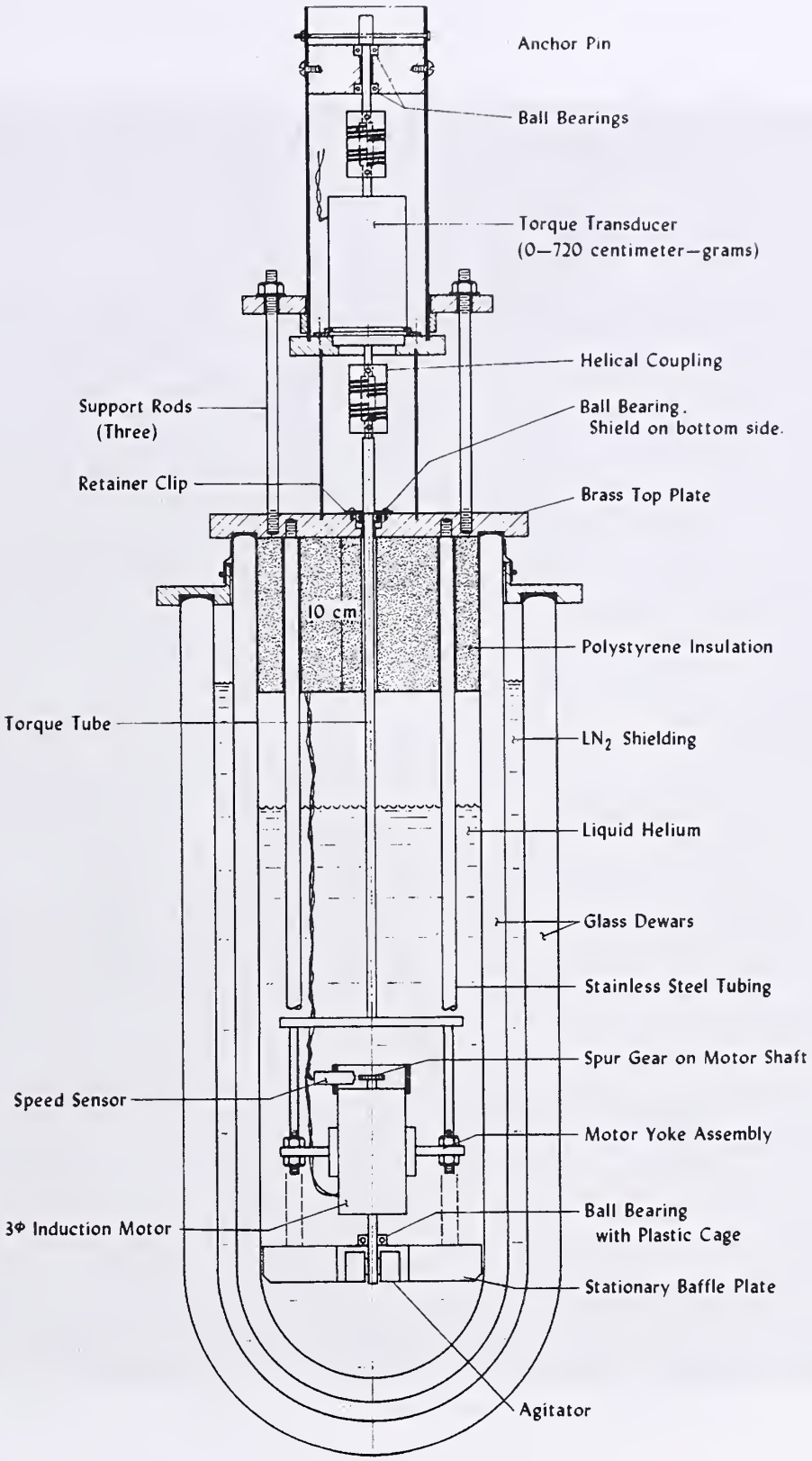

Figure 1. Motor Efficiency Test Apparatus

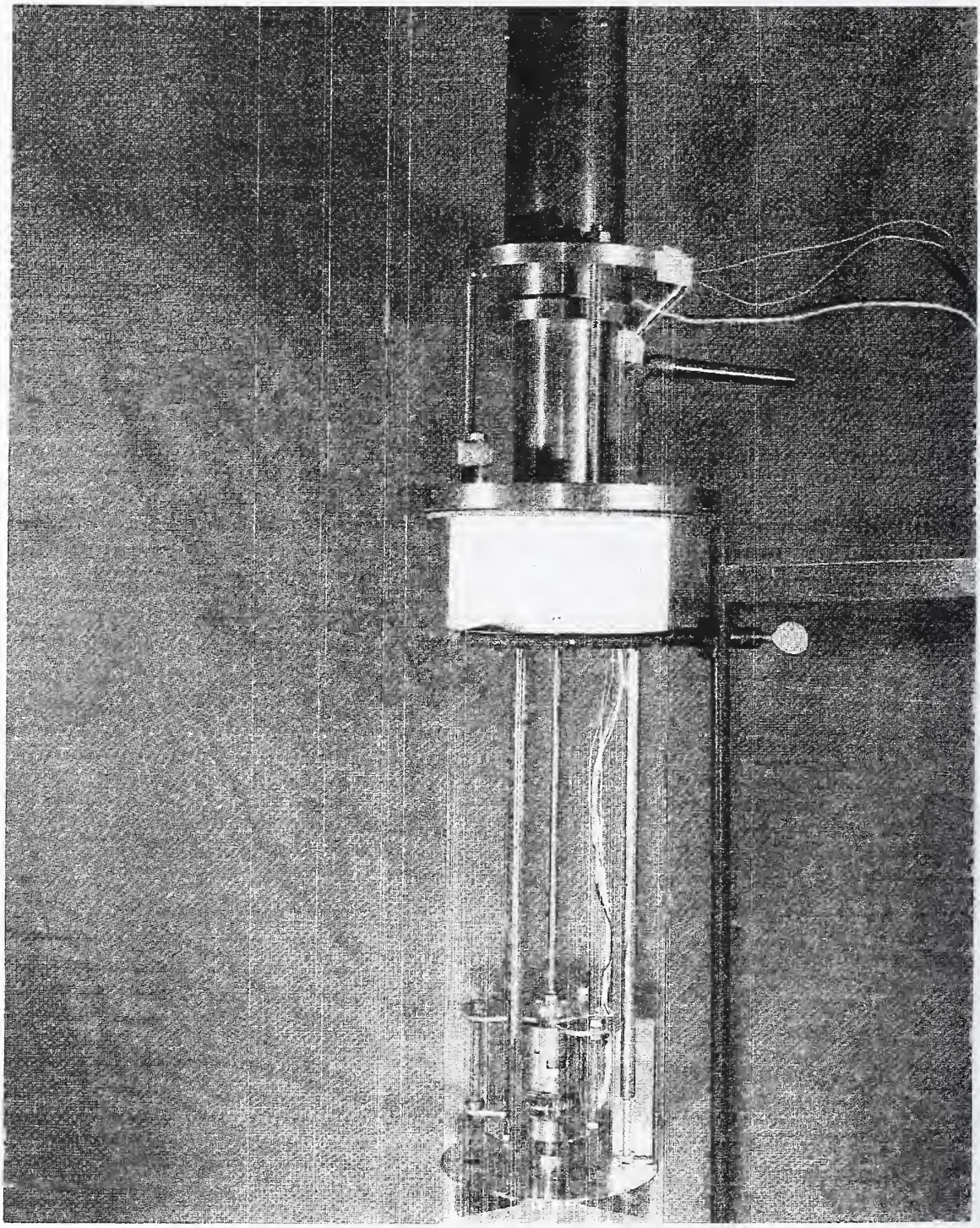

Figure 2. Photo, motor efficiency test apparatus.

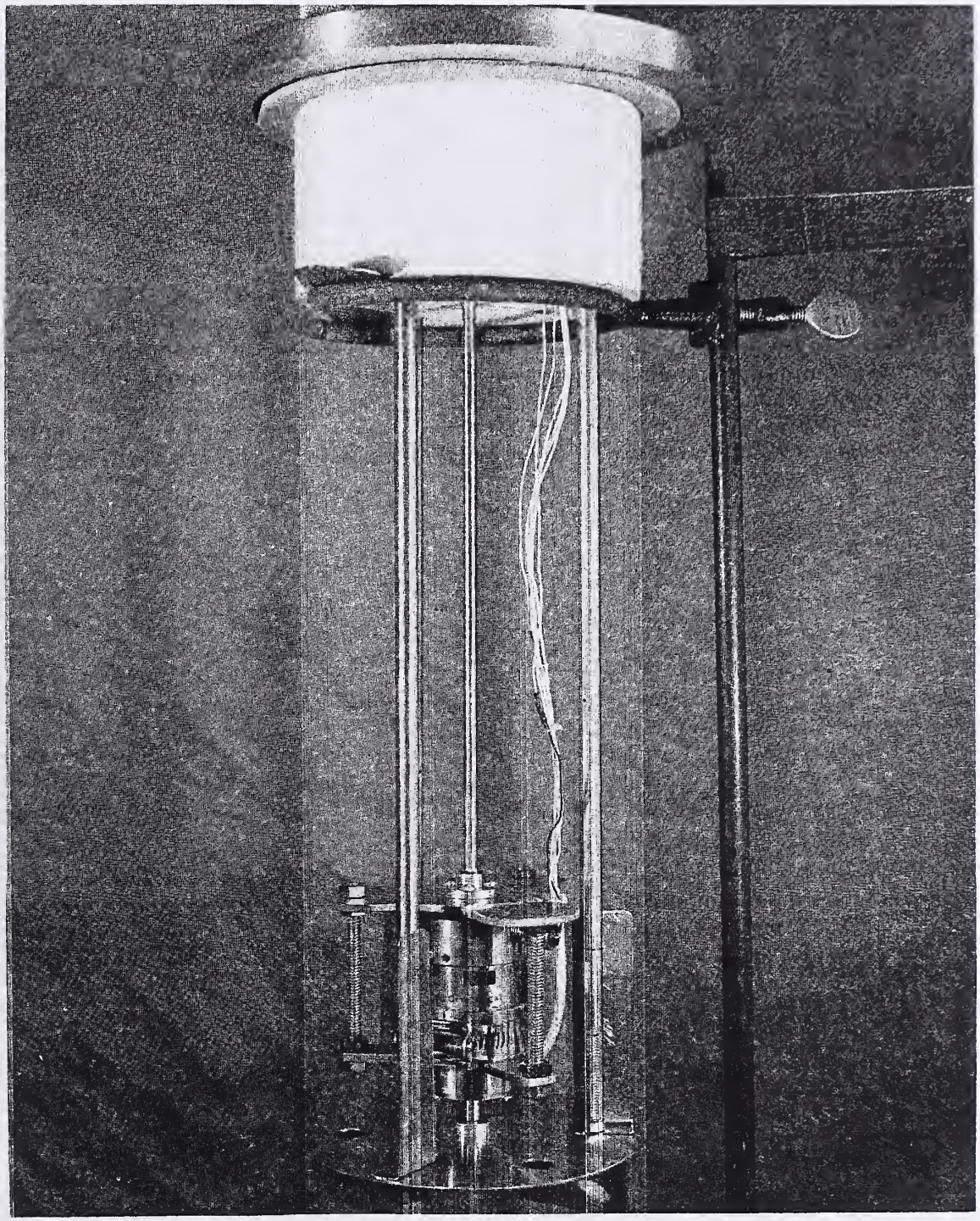

Figure 3. Photo, motor efficiency test apparatus.

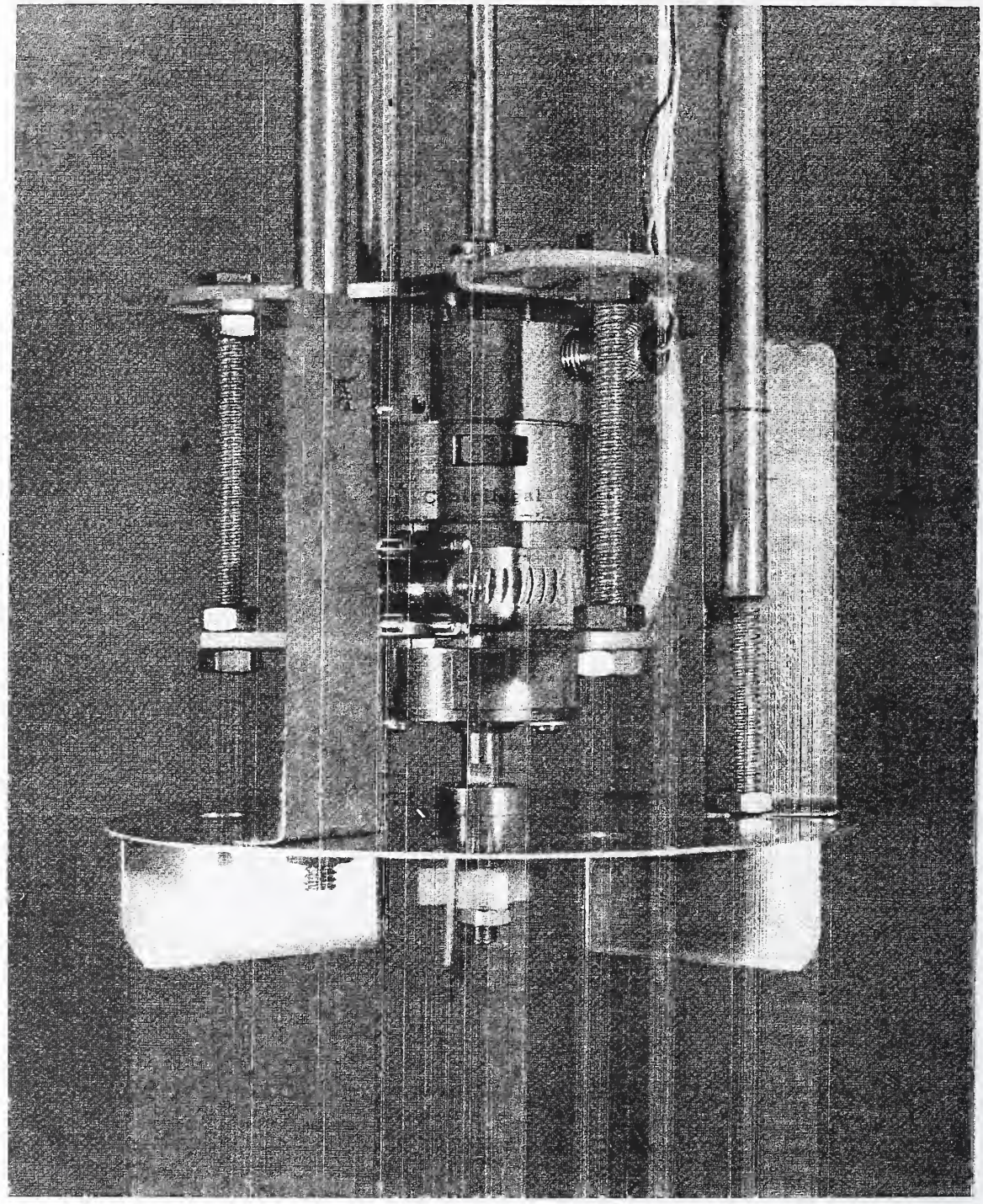

Figure 4. Photo, motor yoke assembly.

motor bearings. The shielding vessel was then filled with liquid nitrogen and the inner vessel subsequently filled with liquid helium. The tests were conducted with the helium liquid level > 6 cm above the yoke assembly. The motor was run at a given 3-phase input frequency of 300, 400 or 500 Hz with line-neutral voltage varying from 20 to 130 volts; efficiency data was taken at each 10 volt increment.

The electrical power into the motor, the motor speed, the torque, and the voltage were recorded for each voltage setting. The net power into the motor, the power out of the motor, and the motor slip were then calculated. Tests were conducted using three different size agitators for varied loading. The zero reading on the torque transducer was checked before and after each individual test, since the wires leading from the yoke assembly to the foam could be a source of error. However, the total movement of the yoke and motor assembly for the maximum 720 centimeter-grams (10 inch-ounces) torque reading is only 0.64 degrees. Since the torque meter returned to zero after each test and the full scale rotation of the motor assembly is so small, the error introduced by the wires is thought to be negligible. The overall accuracy of the measurements is estimated to be ± 3 percent.

A.1.3. Motor Efficiency Test Results

Efficiency tests were conducted in both liquid nitrogen and liquid helium. The efficiency data for liquid helium are shown in figures 5, 6, 7, and 8. Figure 5 is a plot of corrected power input to the motor vs motor slip for an input frequency of 400 Hz using three different agitators on the motor, giving light, medium, and heavy loading. Similar data was obtained for input frequencies of 300 and 500 Hz. If the data are plotted showing motor efficiency versus induction motor slip as in figures 6, 7, and 8, it becomes immediately apparent that the motor operates at maximum efficiency when experiencing slip in the range of 5-10 percent. Also, the peak efficiency of the motor is slightly dependent upon input frequency, and the magnitude of the efficiency is dependent on the load placed upon the motor. With a 3-phase frequency of 400 Hz (the motor design input frequency) the motor has optimum efficiency in the slip range of 5-10 percent. The efficiency of the motor with 8 percent slip and 400 Hz input is 58, 69, and 74 percent for the light, medium, and heavy motor loads, respectively. This is higher than had been estimated (without data) in reference [1].

For most applications where small electric motors might run in liquid helium, it is desirable to operate the motors at or near maximum efficiency in order to boil away a minimum amount of liquid helium. Thus, electric motor efficiencies in the range of 60 to 75 percent are encouraging for applications using electric motors to power small helium pumps to circulate liquid helium in superconducting power transmission cables and other superconducting devices. Even higher efficiencies may be possible with additional innovation.

Efficiency data for similar tests in liquid nitrogen are shown in figure 9. The efficiencies were not as high as in the liquid helium tests, possibly because of the different operating characteristics of the motor at 4 and 76 K. Minimal data were taken at 76 K.

The efficiency data plotted in figures 5, 6, 7, and 8 do not permit a quick determination of the electric motor efficiency for given operating conditions, because the efficiency depends on the motor load which is not quantitatively specified in these figures. However, if the motor efficiency is plotted vs power input/ 3-phase input frequency for a given motor slip, it is possible to quickly determine the motor efficiency for a particular set of operating conditions. Curves are plotted for eight percent slip and eleven percent slip in figure 10. Eight and eleven percent slip are plotted since the motor was run with these two values for slip in the two sets of performance tests with the helium pump. These data were then used to extract the pump efficiency from data on the combined efficiency of the motor and pump.

A.2. Pump Performance Tests

The rather simple helium pump used in these tests was designed by an independent engineering company. The pump bolts directly to the motor as shown in figure 11. The pump has an axial flow inducer, a centrifugal type impeller, and a vaneless diffuser. The pump was specifically designed for liquid helium and has a design point of 15.2 m helium at 2.52×10^{-4} m^3/s (50 ft helium @ 4 gpm) at 6000 rpm.

The pump and motor have been tested previously; the pump performance data are reported in reference [1]. The previous pump performance data fell significantly below the design specifications for the pump.

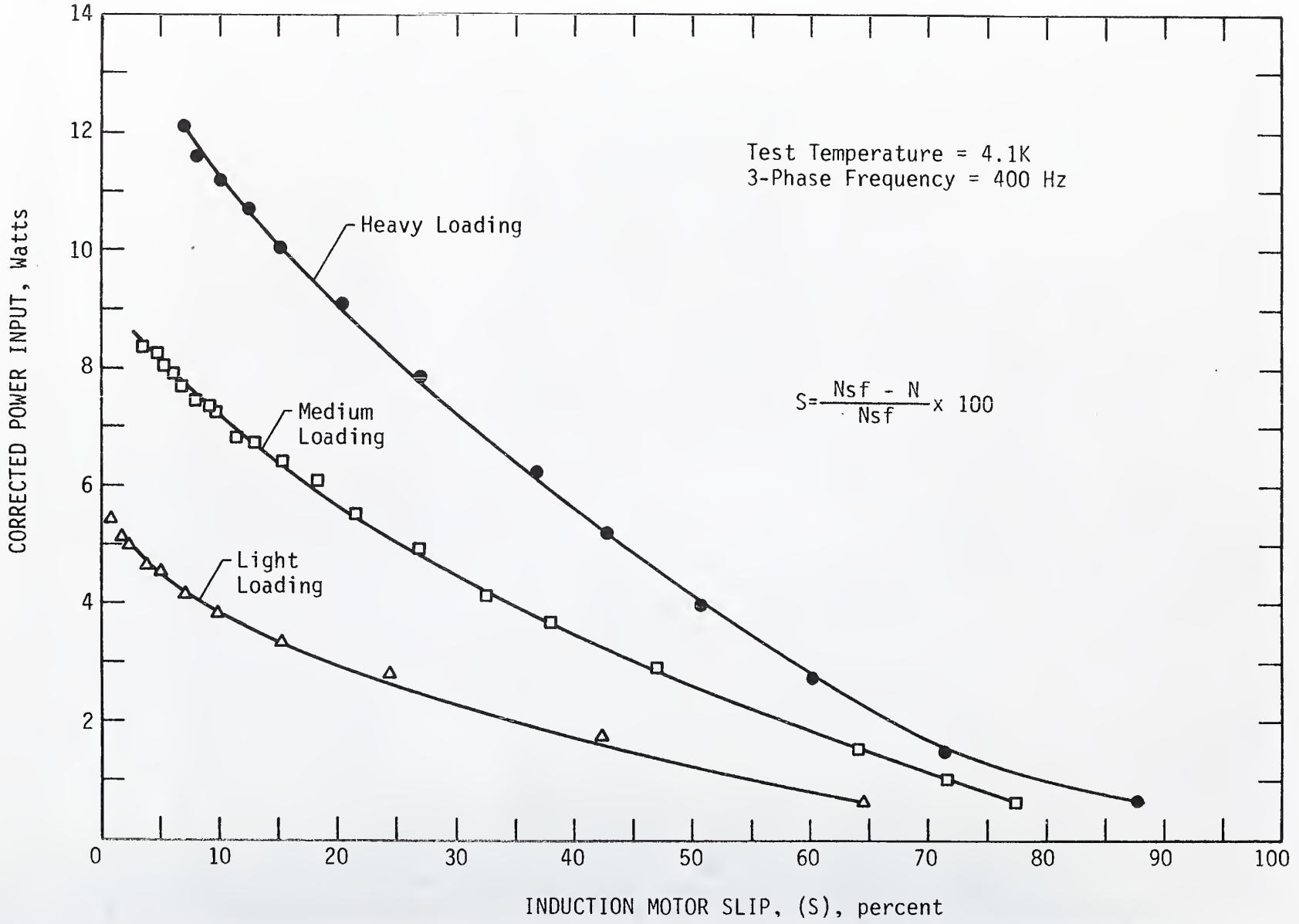

Figure 5. Induction motor load characteristics.

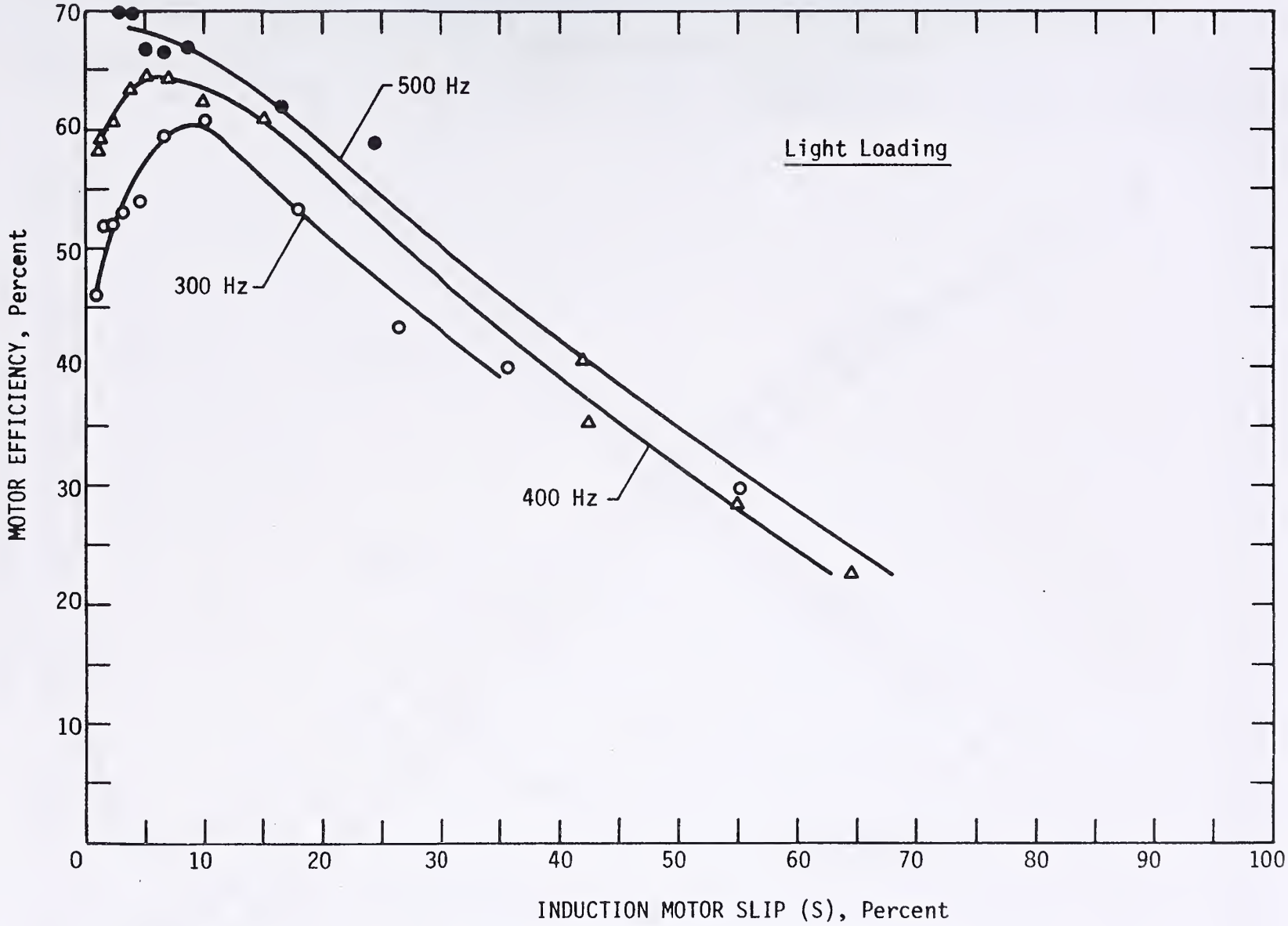

Figure 6. Induction motor efficiency in liquid helium, light loading.

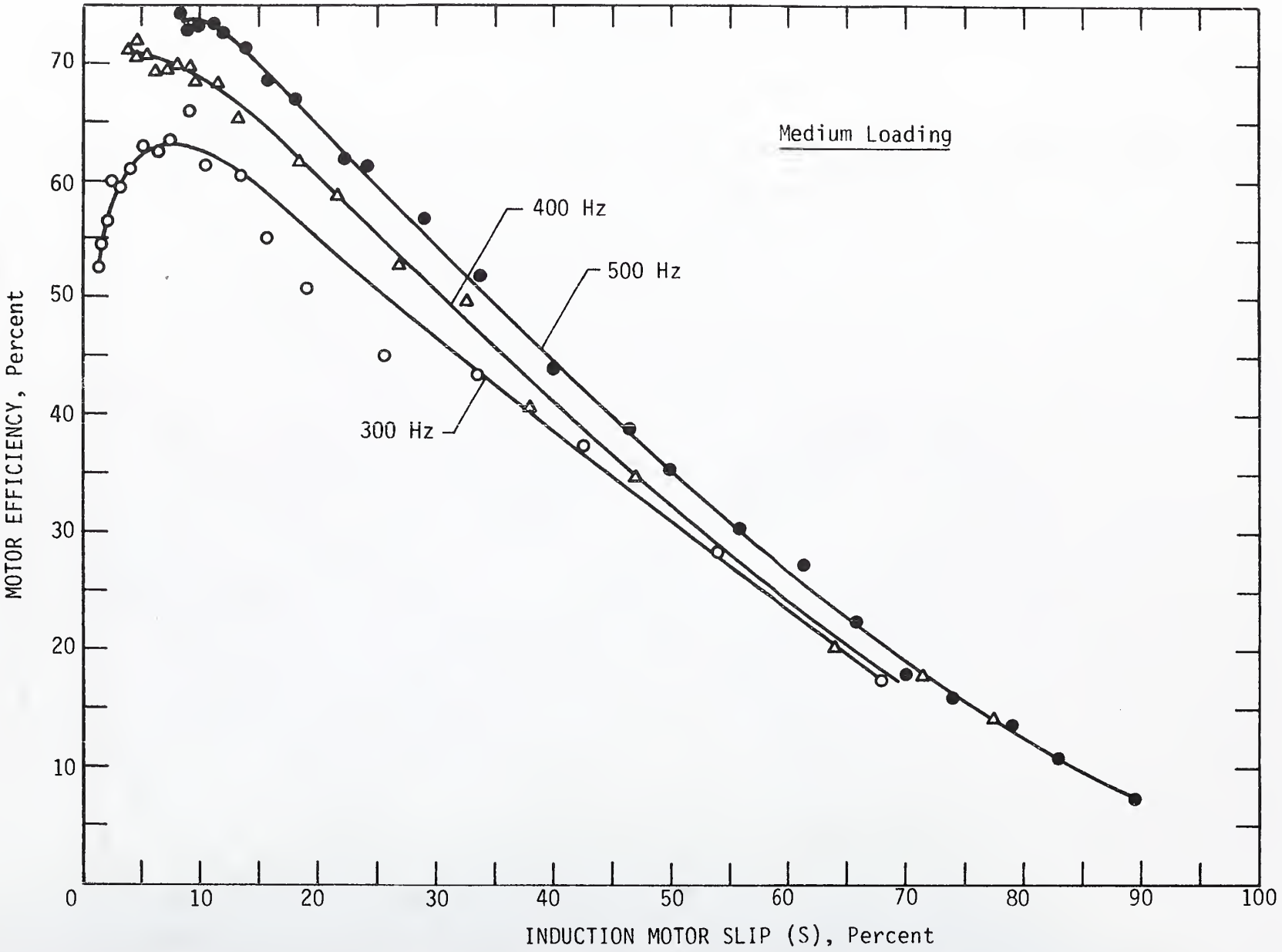

Figure 7. Induction motor efficiency in liquid helium, medium loading.

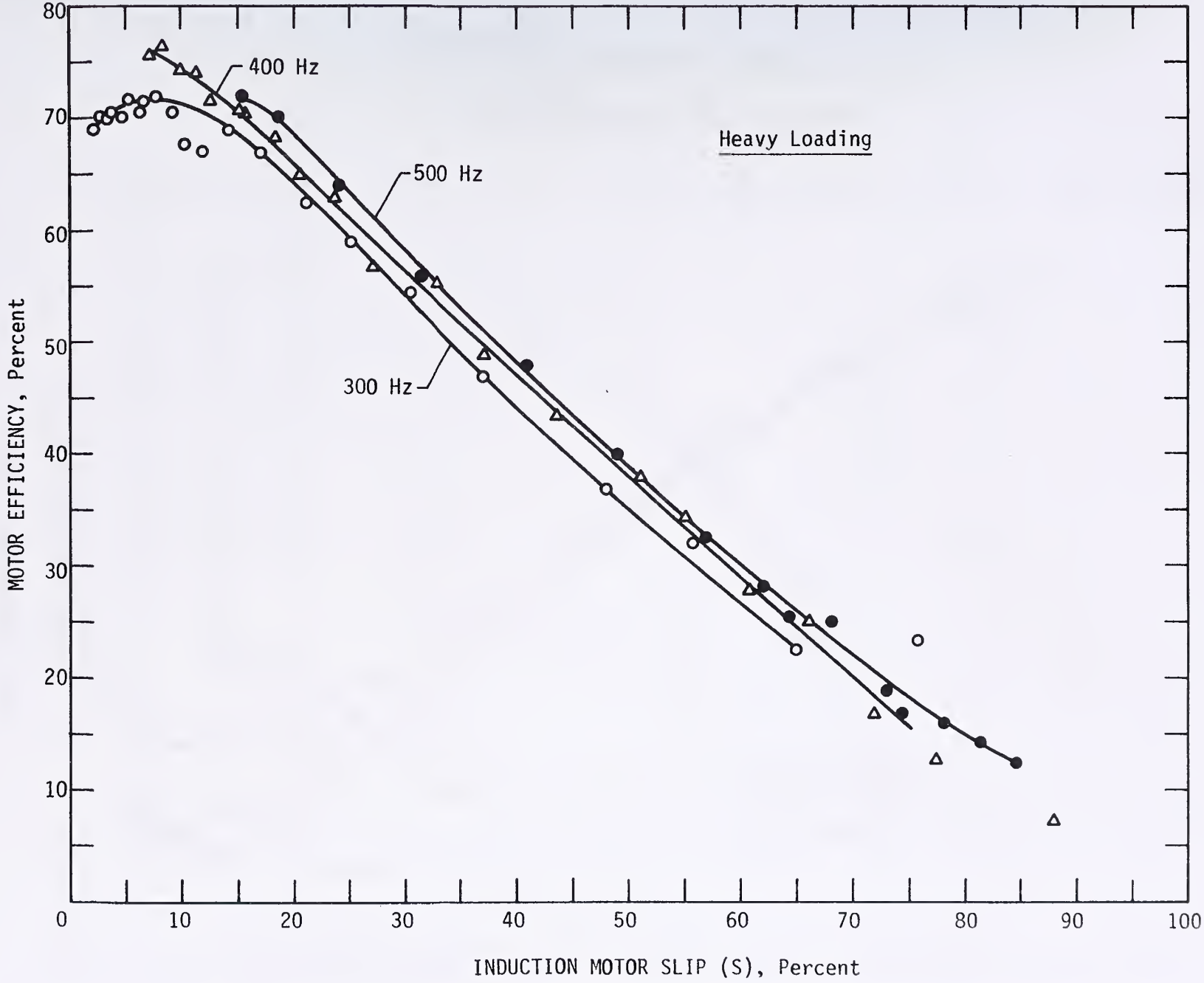

Figure 8. Induction motor efficiency in liquid helium, heavy loading.

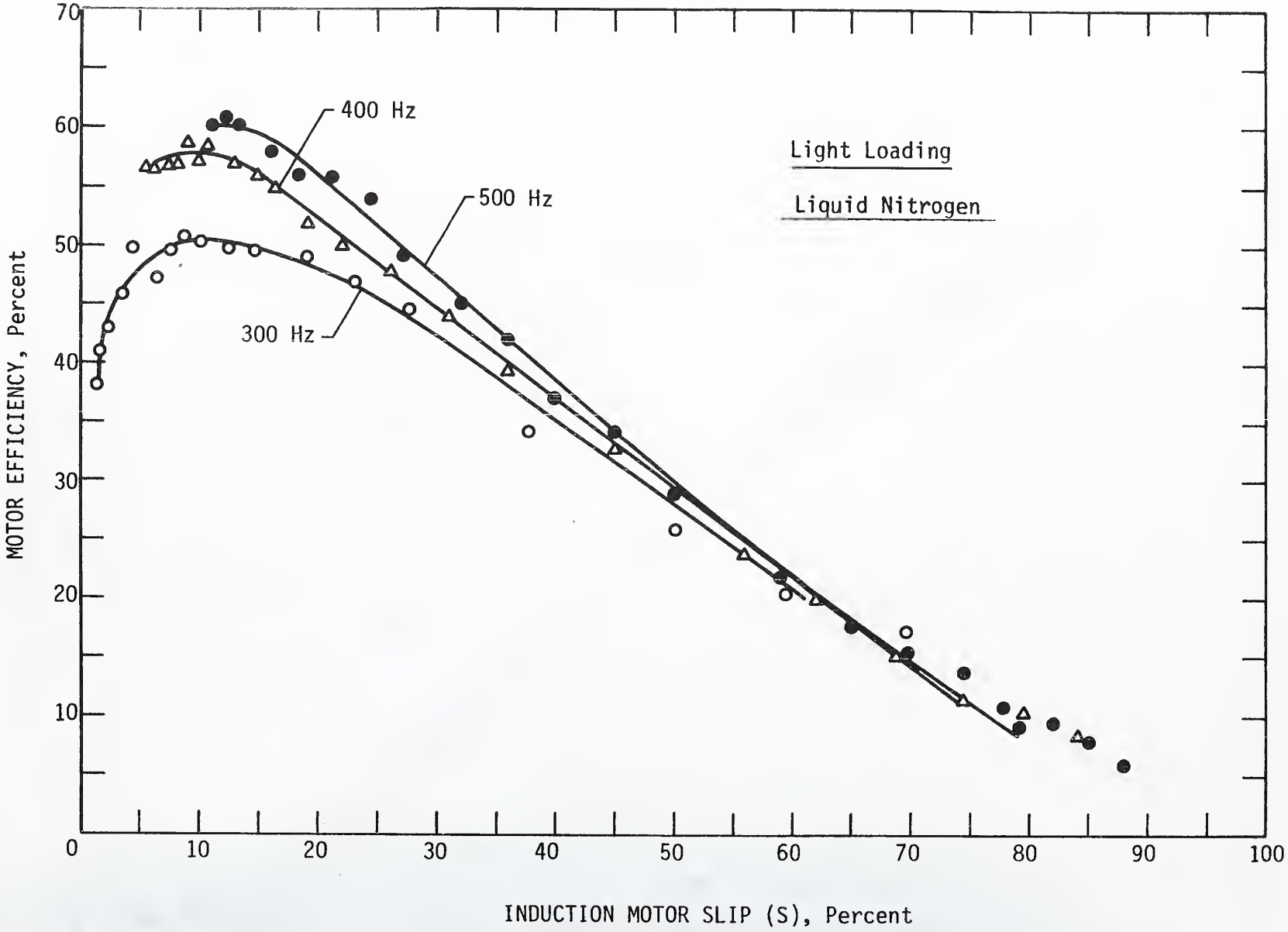

Figure 9. Induction motor efficiency in liquid nitrogen, light loading.

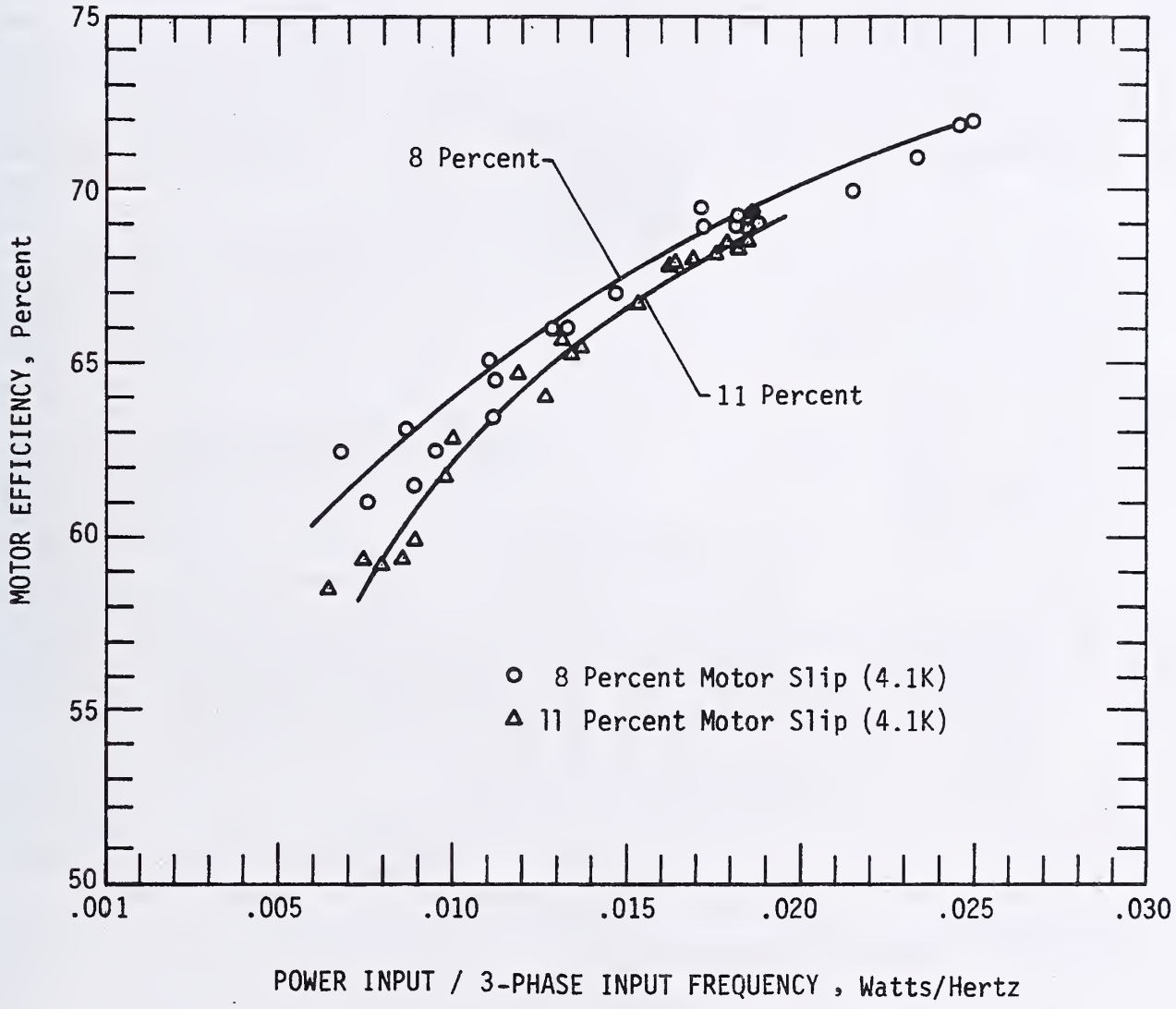

Figure 10. Induction motor efficiency, 8 and 11 percent slip.

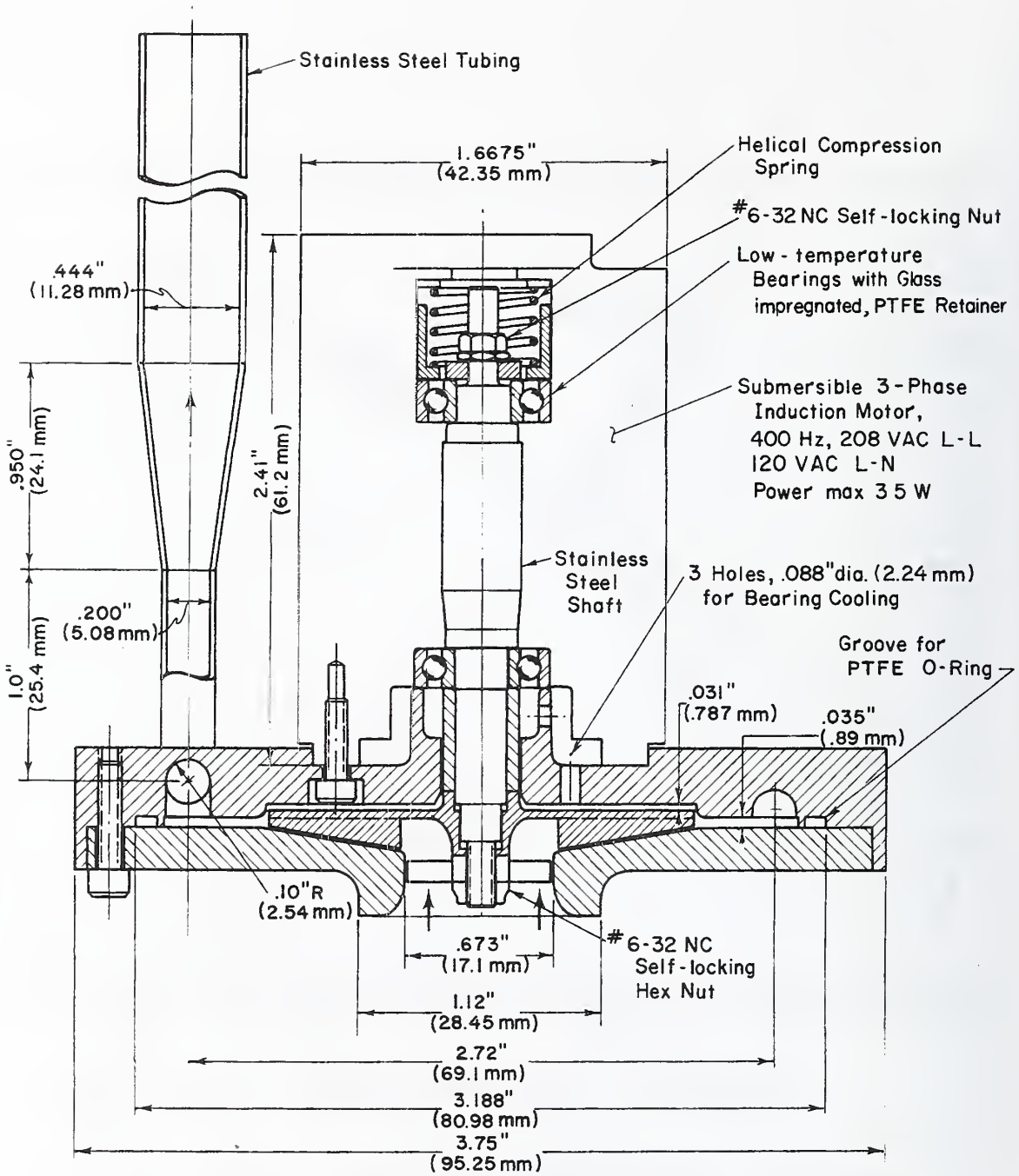

Figure 11. Assembly drawing of the helium pump and the original inlet geometry.

In view of this it was decided that, (1) the impeller position in the pump should be checked, and adjusted if necessary for optimum performance, (2) the inlet geometry to the pump should be streamlined, and (3) comparative tests should be made to determine the effect of the pump motor coolant passages on the performance characteristics of the pump.

The impeller position within the pump was checked. The base of the impeller (i.e., the flat surface where the vanes attach to the disc shaped body) had a $\begin{matrix}+0.203 \text{ mm} \\ -0.102 \text{ mm}\end{matrix}$ $\left\{\begin{matrix}+0.008" \\ -0.004"\end{matrix}\right\}$ variation from the plane of the vaneless diffuser; the variation resulted mostly because the back shoulder of the impeller was not parallel with the impeller base. For optimum performance, the impeller base should be in the same plane as the vaneless diffuser plane. The back shoulder of the impeller was re-machined perpendicular to the axis, reducing the impeller variation to $\begin{matrix}+0.051 \text{ mm} \\ -0.013 \text{ mm}\end{matrix}$ $\left\{\begin{matrix}+0.002" \\ -0.0005"\end{matrix}\right\}$ with respect to the plane of the vaneless diffuser. There was also a slight machining error in the cover plate of the pump. An entirely new pump cover plate was machined with a much improved suction bell inlet. The original acorn shaped hexagonal shaft nut was also replaced with an ogive shaped nut to improve the streamline flow into the pump. The photos of the motor and pump in figures 12, 13, and 14 show the new pump cover plate with the improved suction bell and the streamlined ogive nut on the inducer. A drawing of the impeller is shown in figure 15. After making the above improvements, the pump was again tested for H-Q performance characteristics in liquid helium.

A.2.1. Pump Performance Test Apparatus

The test apparatus used to determine the performance characteristics of the pump is shown in figure 16. The apparatus is essentially the same as used in the previous work [1], except for the turbine flowmeter which was added for the cavitation measurements. The entire pump assembly and flow loop are placed in a dewar filled with liquid helium. The liquid helium level is always maintained above the level of the flow control valve. The helium flow path is as shown: entering the bottom of the pump, discharging vertically through the venturi flowmeter and on through the turbine type flowmeter, then through the discharge control valve and on down through a conical diffuser to the helium bath in the dewar. The discharge control valve is used to manually adjust the rate of flow through the pump. The venturi meter and the turbine meter both measure the flow rate of the pump. The flow rate through the venturi is determined from the ΔP measurement across the meter and a calibration factor. The turbine type flowmeter is calibrated using the venturi meter.

The pressure lines from the test apparatus are stainless steel capillary tubing (1.57 mm OD x 0.2 mm wall). The capillary tubes were thermally connected every 20 cm to maintain approximately the same thermal gradient within each tube, thus minimizing the liquid level (head) differences within the various capillary tubes. This procedure was found to be necessary to minimize random drifts and fluctuations in the venturi ΔP readings. The pressure lines exit to ambient temperature diaphragm type ΔP gauges.

The capacitance type liquid level gauge used during the earlier tests was replaced with a superconducting type liquid level gauge with improved sensitivity and resolution. The improved liquid level sensor was necessary because we planned to run cavitation tests at 4.7 K, where the density ratio of liquid to vapor is only 4.17, making a capacitance type liquid level indicator very marginal (see part B).

A barostat was used to control the ullage pressure of the helium dewar, thus controlling the temperature of the liquid helium bath. The remainder of the instrumentation — the 3-phase power supply, the polyphase wattmeter, the pump and motor speed counter were described previously in section A.1.1.

A.2.2. Pump Performance Test Procedure

Previous to conducting a test, the helium dewar was evacuated and subsequently pressurized to near atmospheric pressure using helium gas. This cycle was repeated three times in order to minimize condensible gas impurities and moisture within the experimental vessel. The nitrogen shielding dewar would then be filled, and subsequently the experimental dewar would be filled with liquid helium to $\sim$ 40 cm above the level of the flow control valve.

At the start of a test, the barostat would be adjusted, the predetermined 3-phase input frequency would be set so the motor would operate with the desired slip, and the motor or pump speed would be adjusted to the desired speed by adjusting the input voltage.

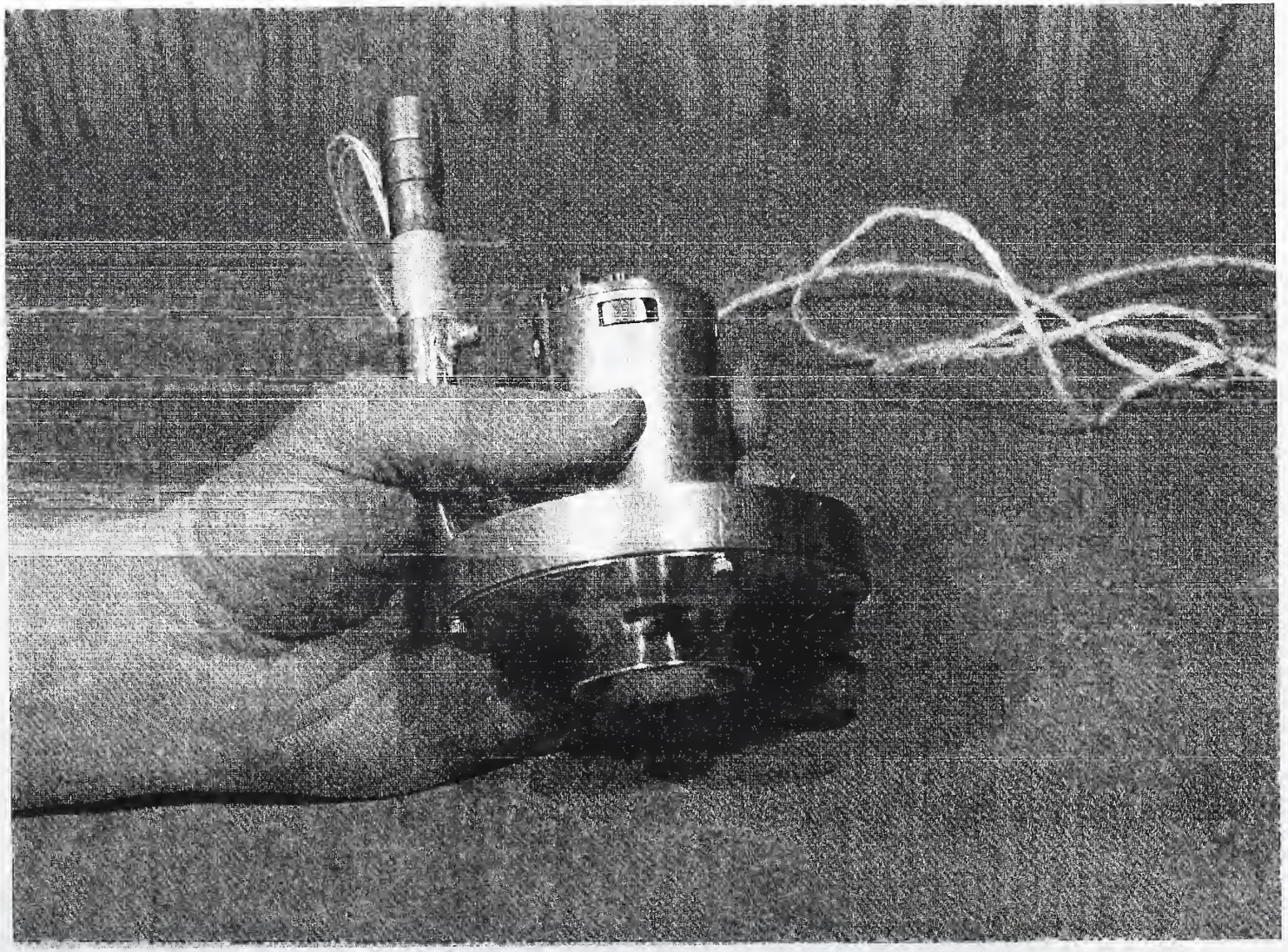

Figure 12. Photo, pump and motor assembly.

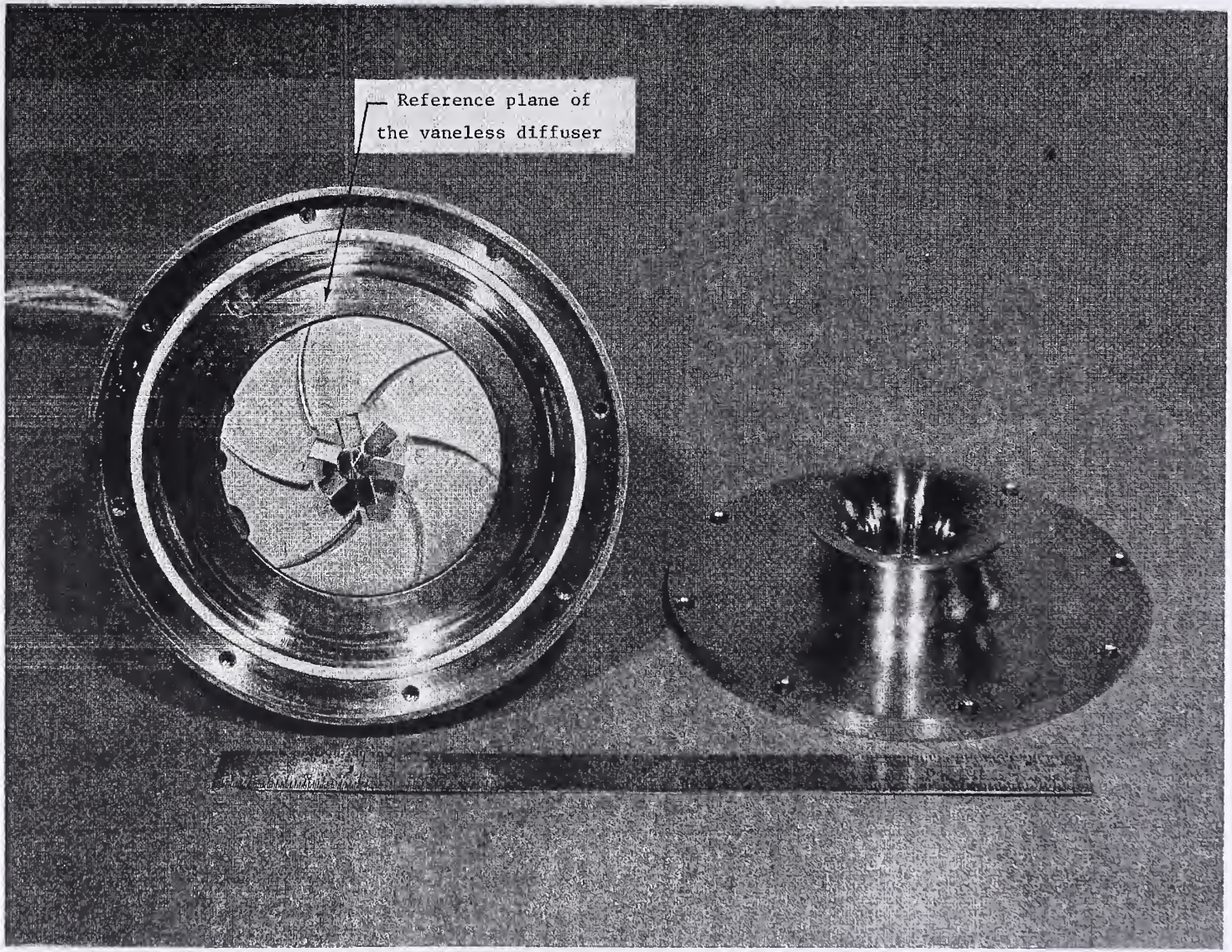

Figure 13. Photo, pump interior.

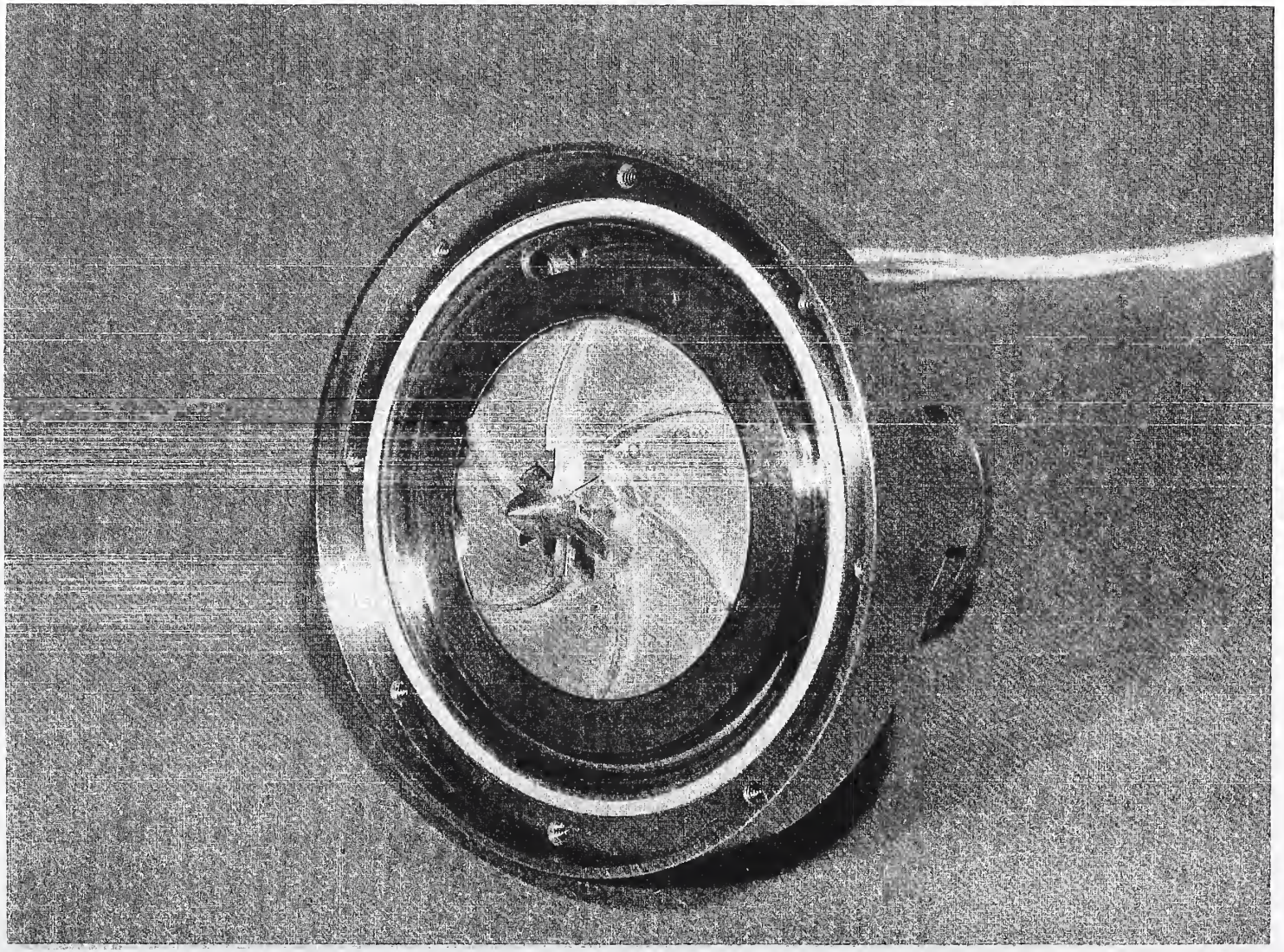

Figure 14. Photo, pump inducer, impeller, and vaneless diffuser.

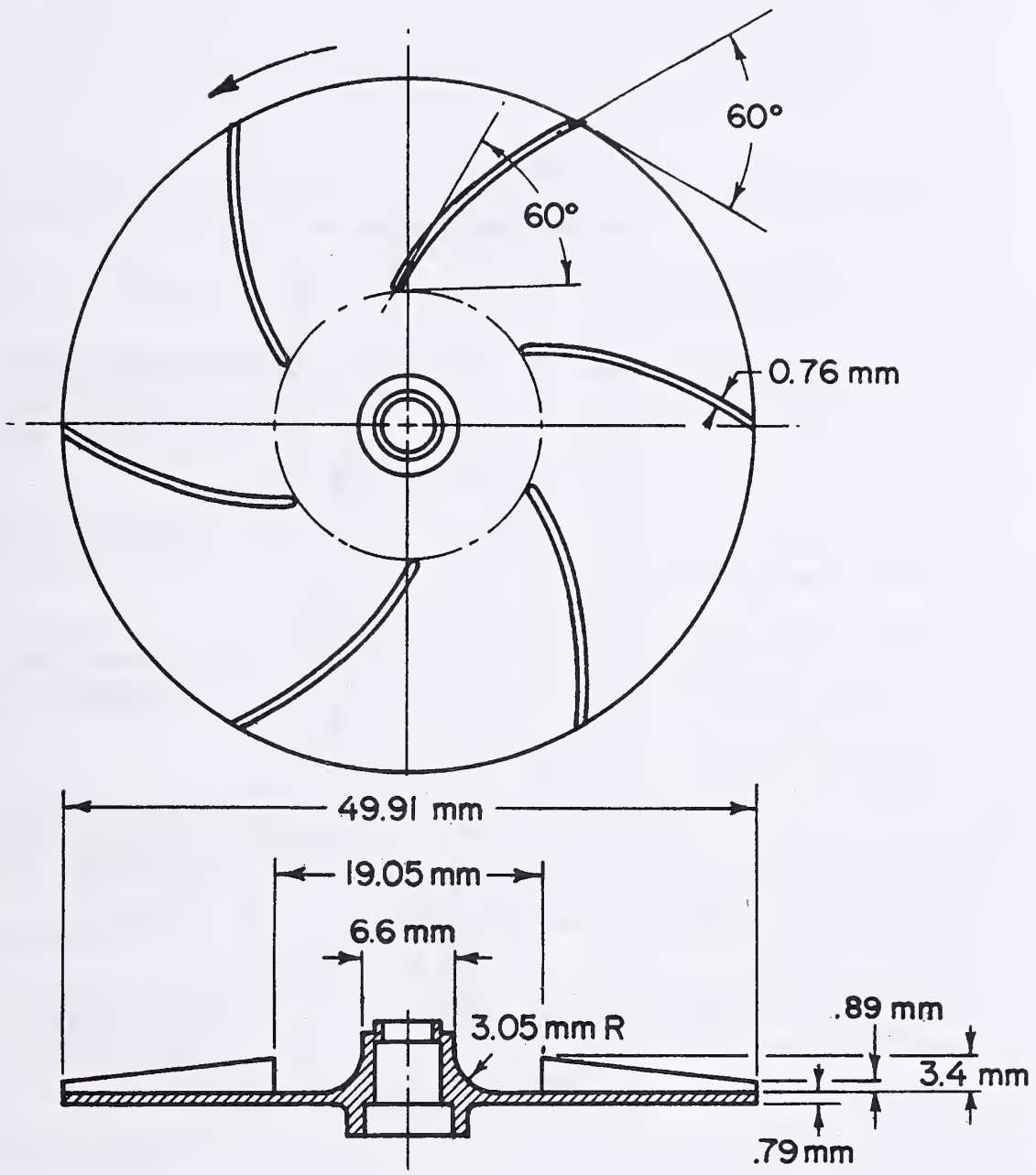

Figure 15. Centrifugal impeller for helium pump.

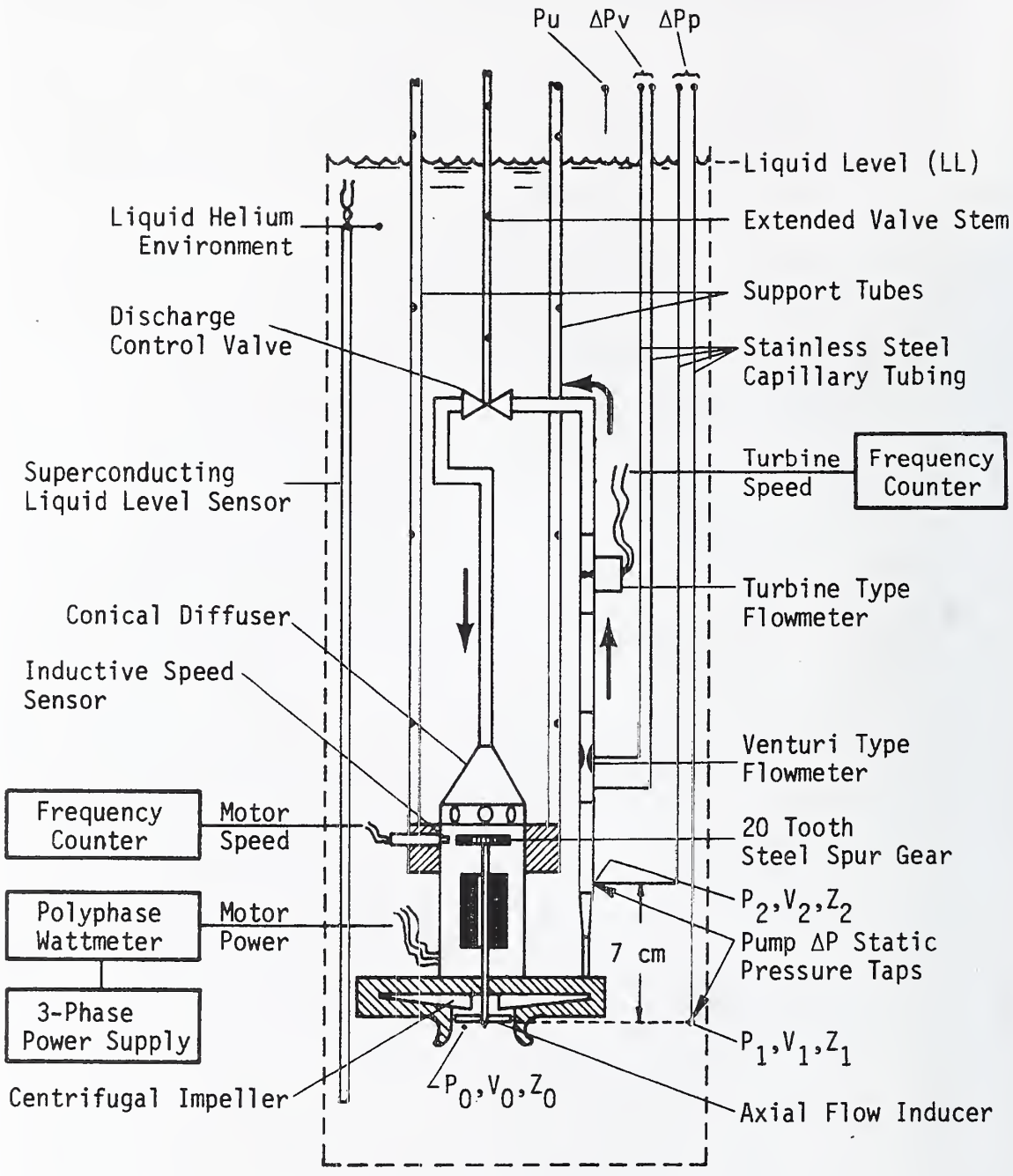

Figure 16. Helium pump test loop and instrumentation.

When the desired operating conditions were achieved, the following data were recorded: the ullage pressure, the pump ΔP, the venturi meter ΔP, the pump speed, the liquid level, the line-neutral volts, the power into the motor, the 3-phase frequency input, and the turbine meter signal. After recording the above data for a given flow rate, the flow rate would be changed by manually adjusting the flow control valve, the pump speed would be readjusted, and another set of data would be recorded. By adjusting the flow control valve in increments between the closed and open positions, pump performance data were obtained for the full flow range. During the pump performance tests, the liquid helium level was always maintained at least 4 cm above the level of the flow control valve.

A.2.3. Pump Performance Results

The total dynamic head (H) of the pump was calculated in the conventional manner; however, the measurement procedure should be carefully explained. The total dynamic head is normally defined as

$$H = \frac{1}{g} \int_o^2 \frac{dP}{\rho} + \frac{V_2^2 - V_o^2}{2g} + (Z_2 - Z_o). \qquad (1)$$

If we assume that, in our particular case, the flow is isothermal and the fluid is of negligible compressibility, reference [1]

$$\frac{1}{g} \int_o^2 \frac{dP}{\rho} = \frac{P_2 - P_o}{\rho g},$$

and

$$H = \frac{P_2 - P_o}{\rho g} + \frac{V_2^2 - V_o^2}{2g} + (Z_2 - Z_o). \qquad (2)$$

Referring to figure 16, $Z_o = Z_1$ and thus $Z_2 - Z_o = Z_2 - Z_1$. P_o is the static pressure at the pump entrance and P_1 is the static pressure at the same elevation out in the helium bath.

Considering the pressures at points (1) and (2),

$$\frac{P_1}{\rho g} + \frac{V_1^2}{2g} = h_\ell + \frac{P_o}{\rho g} + \frac{V_o^2}{2g}.$$

If V_1 is considered negligible because of the low fluid velocity at point (1), and the pump entry losses are negligible, as with the streamline entry plate,

$$\frac{P_o}{\rho g} = \frac{P_1}{\rho g} - \frac{V_o^2}{2g},$$

and the total dynamic head may be expressed as follows, using variables pertaining to points (1) and (2):

$$H = \frac{P_2 - P_1}{\rho g} + \frac{V_2^2}{2g} + (Z_2 - Z_1). \qquad (3)$$

Next consider the type of instrumentation and methodology used for measuring P_2 and P_1. As shown in figure 16, the pressure taps at points (1) and (2) are connected to a ΔP gauge with stainless steel capillary tubing, and it is assumed that each tube is filled with liquid helium to the same level as the bath liquid level. The relationship between the static pressures at P_1 and P_2 and the gauge pressures P_{2g} and P_{1g} are as follows,

$$P_1 = P_{1g} + \rho g(LL - Z_1) \text{ and } P_2 = P_{2g} + \rho g(LL - Z_2)$$

$$P_2 - P_1 = P_{2g} - P_{1g} + \rho g(LL - Z_2 - LL + Z_1), \text{ or}$$

$$\frac{P_{2g} - P_{1g}}{\rho g} = \frac{P_2 - P_1}{\rho g} + (Z_2 - Z_1) \qquad (4)$$

Thus, using this method of pressure instrumentation, the pressure head calculated using pressures read on the gauge is equal to the actual pressure head developed by the pump between points (1) and (2), plus the elevation head $(Z_2 - Z_1)$, and the total dynamic head of the pump may be expressed in terms of the direct measured or calculable values, thus

$$H = \frac{P_{2g} - P_{1g}}{\rho g} + \frac{V_2^2}{2g} \quad . \tag{5}$$

Pump performance data were taken at 4000, 5000, 6000, and 7000 rpm. The performance data are plotted in figure 17, along with the performance data for 6000 and 7154 rpm taken prior to making the pump improvements. As shown in the figure, the improvements to the pump had a significant effect on the head-capacity performance of the pump. At high flow rates, there is a 30 percent increase in developed head at 6000 rpm. This percentage decreases appreciably at the lower flow rates. However, the pump performance at 6000 rpm is still significantly below the predicted design point plotted in the figure. The pump doesn't even meet design point specifications when operated at 7000 rpm. We have no certain explanation for this discrepancy, which was discussed also in reference [1]. Because in this work we have determined that the pump efficiency is reasonable (about 45%, maximum) we suspect that the failure to meet the stated design specifications is not due to any unusual losses or leakage within the pump, but rather may be due to an analytical error in the original design.

After obtaining one set of performance data with liquid helium, the three motor coolant passages in the top of the pump were plugged in order to determine if these passages have any effect on pump performance. These holes are 2.24 mm diameter and have a total area of 0.116 cm^2. However, the holes are not the only flow path between the pump and the motor; there is an annular space between the rotating shaft and the pump housing. The shaft clearance is 0.43 mm and the cross-section area of the annular flow path is 0.125 cm^2, just slightly larger than the area of the plugged coolant holes. Thus, plugging the three coolant holes eliminated 48 percent of the total area available for liquid helium flow up through the motor.

The pump performance data taken after plugging the motor coolant holes is also plotted in figure 17. The H-Q performance of the pump appears to be the same as previous with the coolant holes open, and one can easily conclude that the coolant passages have no perceivable effect on the head-capacity performance of the pump.

During the later cavitation testing the axial flow inducer was removed from the pump. A set of head-capacity data were taken with the inducer removed; these data are also shown in figure 17. Removing the inducer has little effect on the head developed at high flow rates. Below 1×10^{-4} m^3/s the head decreases significantly as shown.

A.2.4. Pump Efficiency Results

Two different series of liquid helium tests were conducted; one series with the motor coolant holes in the pump open and the motor operating at 11 percent slip, and a later series with the motor coolant holes plugged and the motor running near peak efficiency at 8 percent slip. Since the coolant holes have no effect on pump performance, we have essentially one series of tests with the motor running slightly off peak efficiency at 11 percent slip, and another series of tests with the motor running near peak efficiency at 8 percent slip. Complete performance data for the 6000 rpm tests were plotted from each series. The fluid power, total efficiency, motor efficiency, pump efficiency, power input, and the total dynamic head are plotted for each test. The data is presented in figures 18 and 19. Performance data for the pump and motor at 5000 and 7000 rpm are also shown in figures 20 and 21.

The input power to the system is simply the polyphase wattmeter reading less the necessary correction for the power consumed in the wattmeter measuring circuitry. The power output or fluid power is calculated as follows:

$$\dot{W}_f = \dot{m}gH$$

where $\dot{W}_f$ is watts, $\dot{m}$ is mass flow rate (kg/s), g is the local acceleration of gravity (m/s^2), and H is the total dynamic head (m). The total efficiency is the ratio of the fluid power from the pump to the power into the motor.

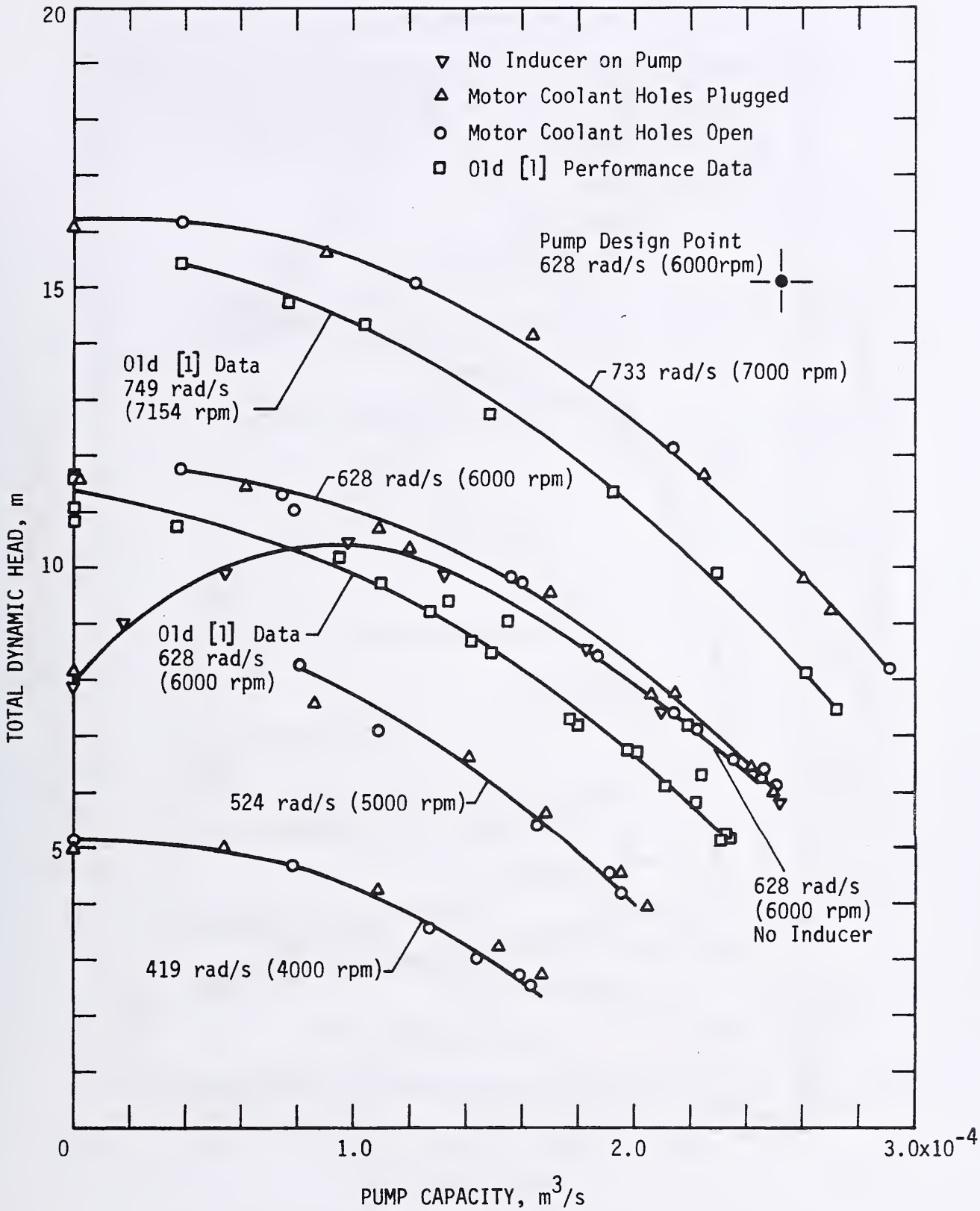

Figure 17. Pump H-Q performance in liquid helium at 4.1 K.

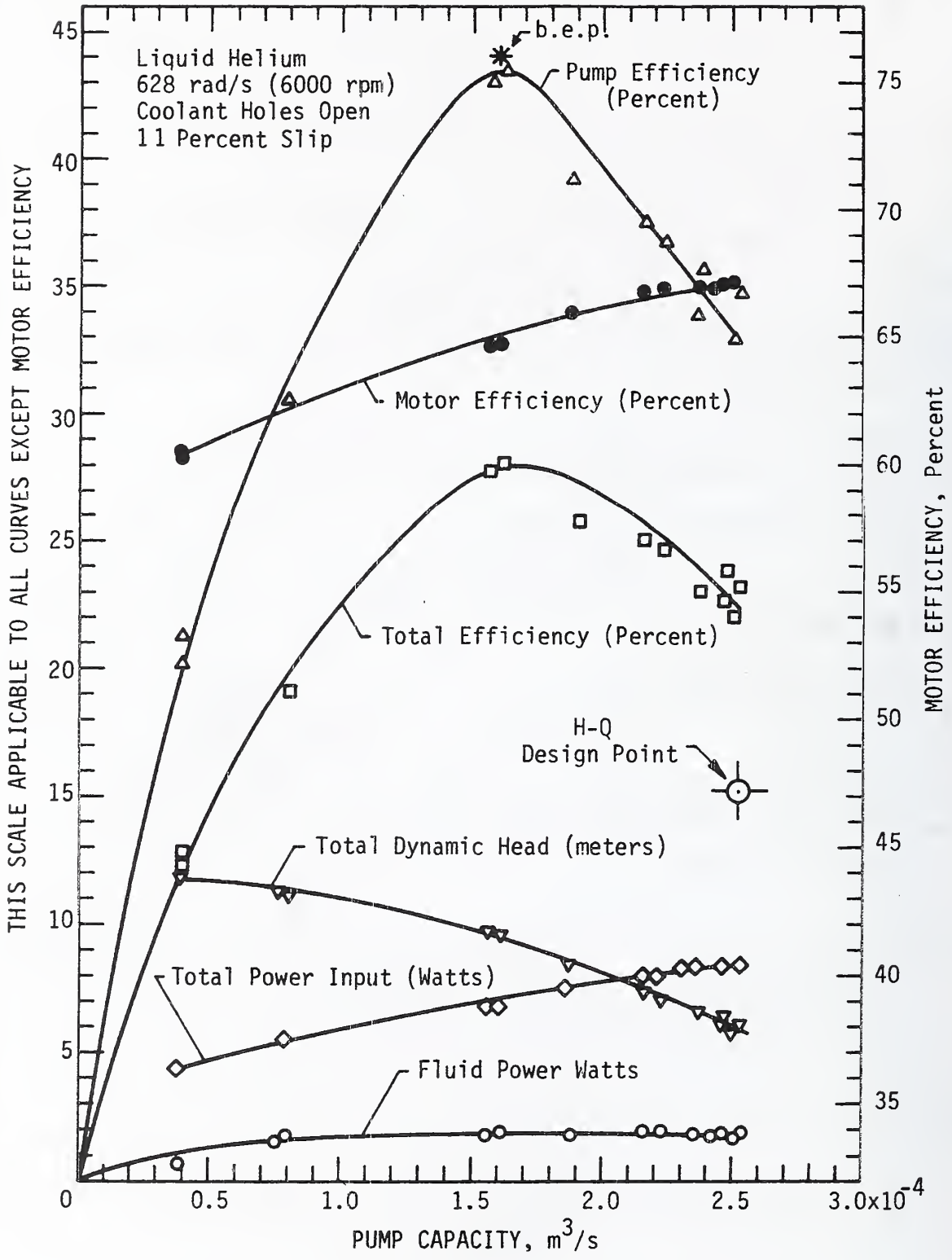

Figure 18. Pump performance, 6000 rpm, 11 percent slip, coolant holes open.

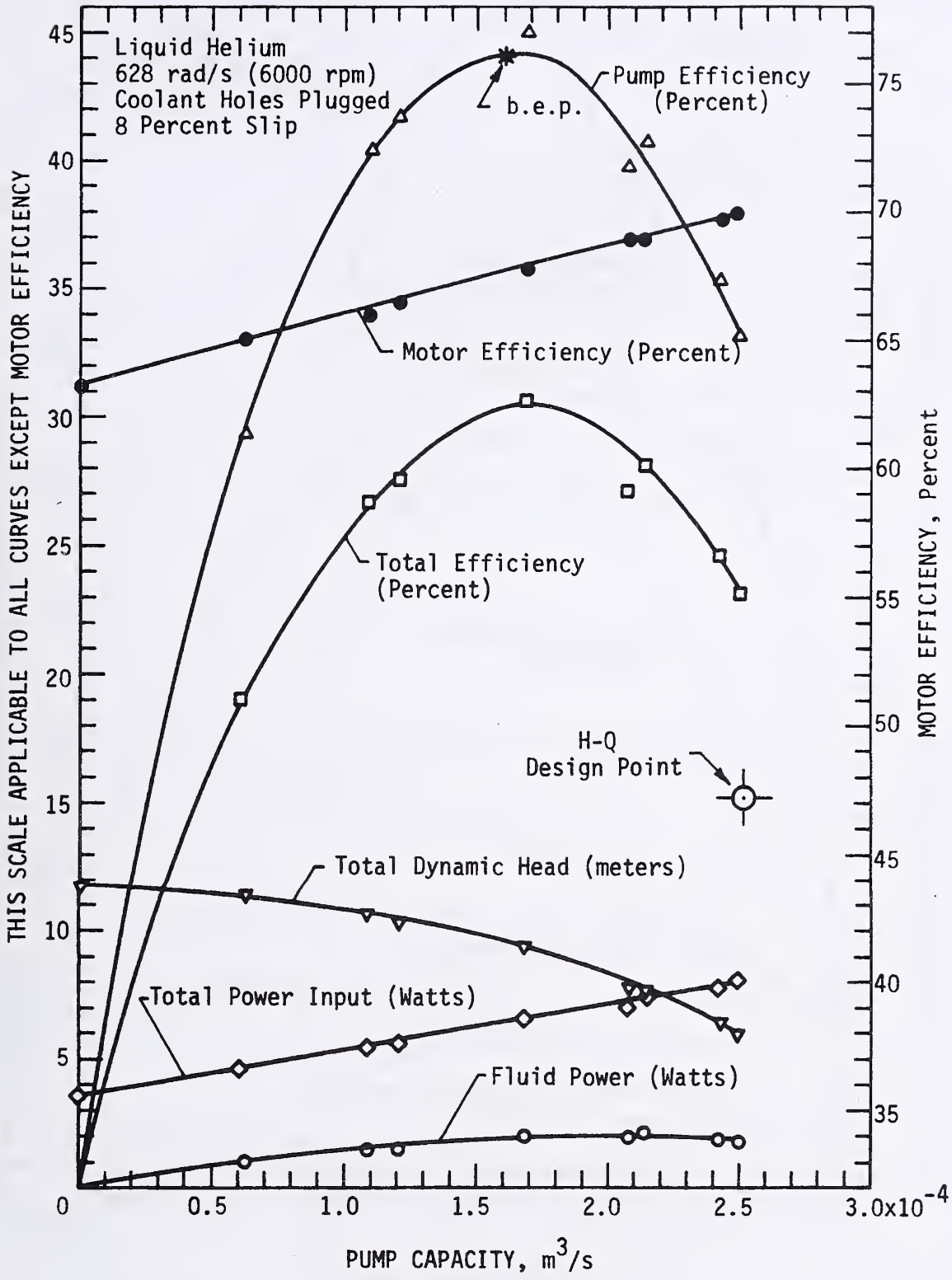

Figure 19. Pump performance, 6000 rpm, 8 percent slip, coolant holes plugged.

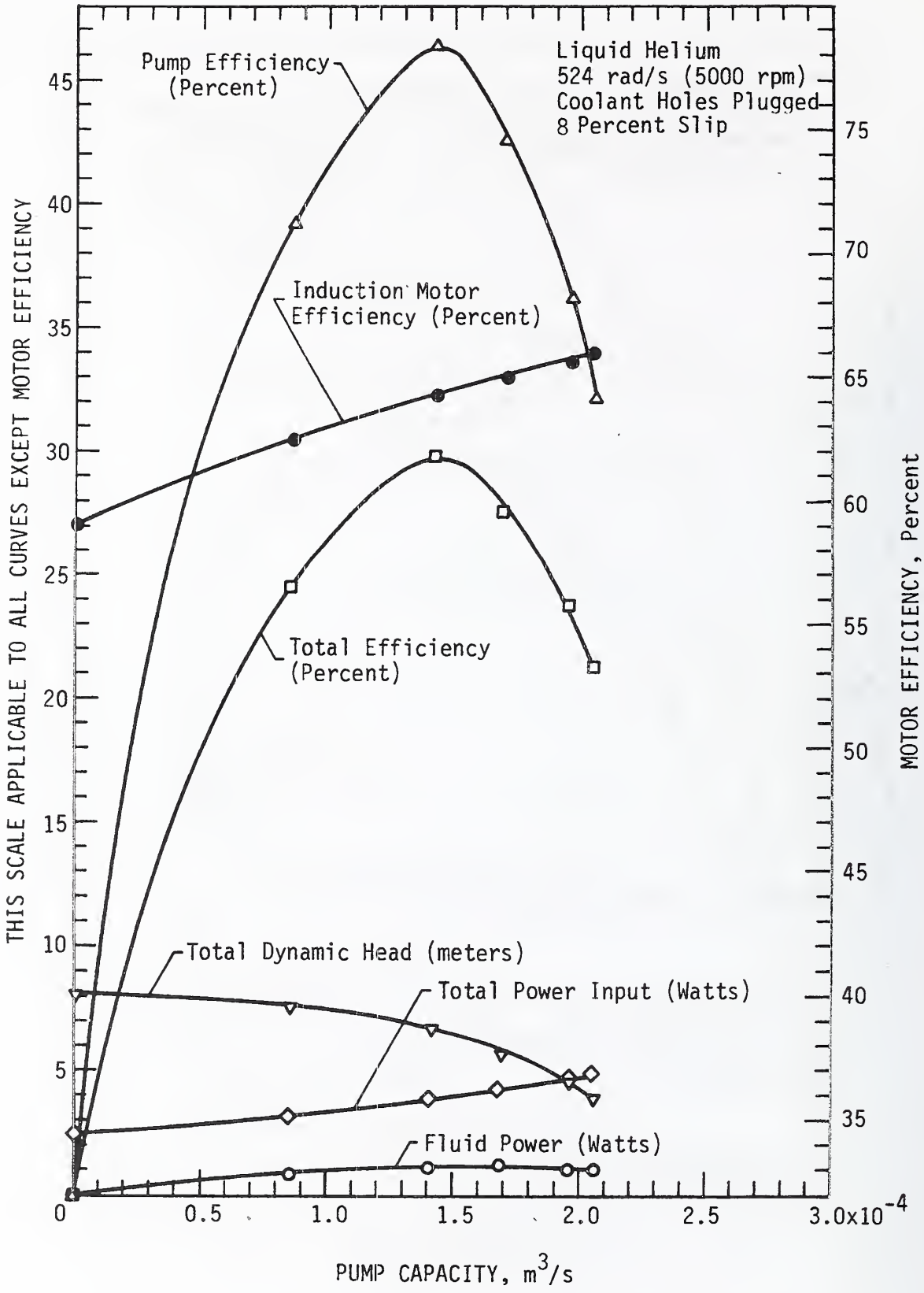

Figure 20. Pump performance, 5000 rpm, 8 percent slip, coolant holes plugged.

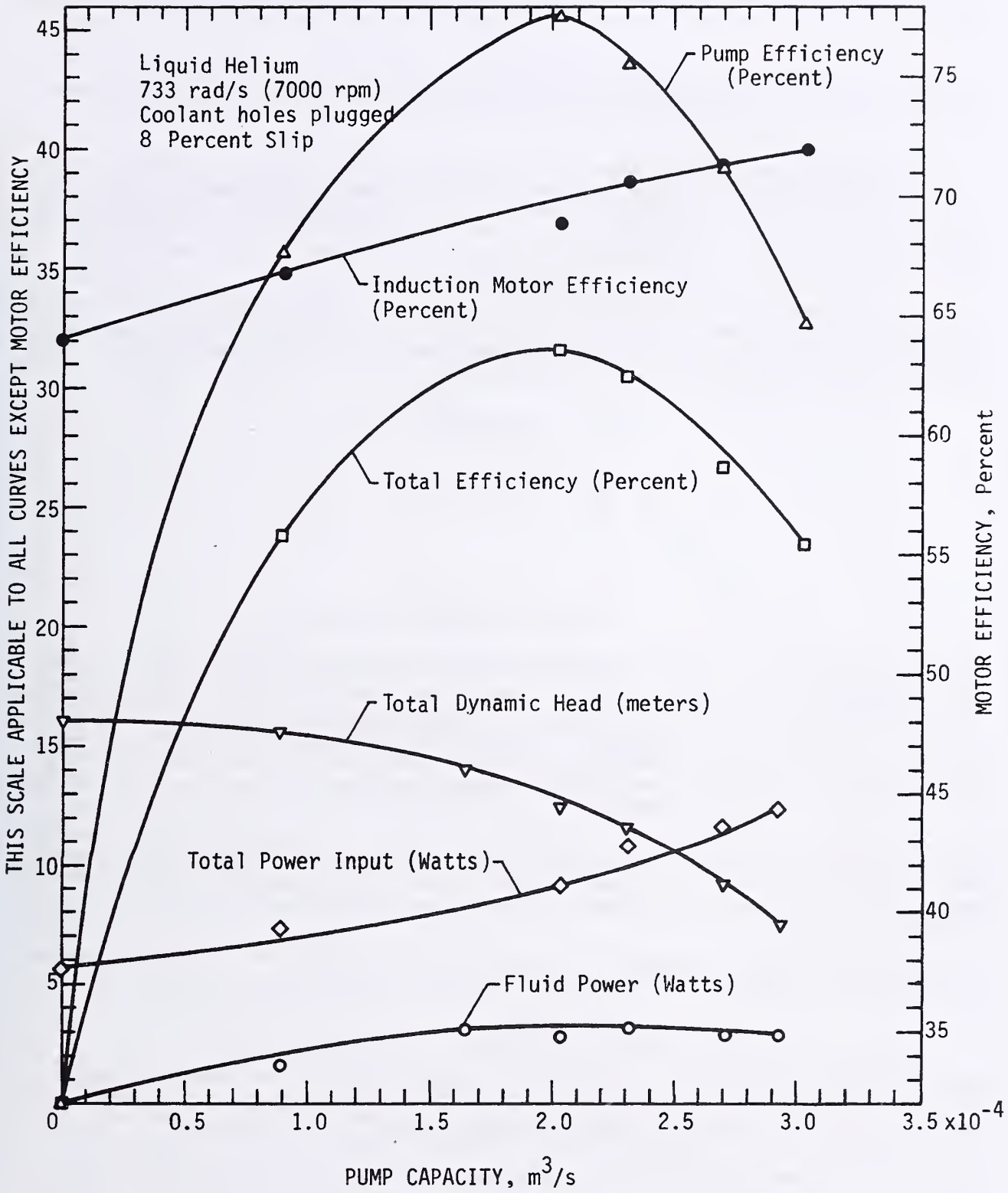

Figure 21. Pump performance, 7000 rpm, 8 percent slip, coolant holes plugged.

The motor efficiency was obtained from the test data described in section A.1.3. The pump efficiency was calculated using the total efficiency and motor efficiency values as,

$$\eta_p = \frac{\eta_t}{\eta_m} \quad .$$

Tabulated values for the pump performance test are presented in table 1. The estimated uncertainty of the pump performance data is ± 5 percent.

Comparing the performance parameters in figures 18 and 19, the total dynamic head for the two tests are essentially the same, and the fluid power is essentially the same. The power input to the motor is higher for the test run at 11 percent slip than for the test run at 8 percent slip. The motor efficiency and consequently the total efficiency is higher when the motor is run at 8 percent slip. The pump efficiencies are the same of course, since the same pump is running at the same speed.

The variation of total dynamic head, pump capacity, and pump shaft power with the speed of a centrifugal pump follow definite relationships known as the pump affinity laws, which may be derived using general principles of similitude. The affinity laws for a given centrifugal pump are expressed by the following equations:

$$\frac{Q}{Q_1} = \left(\frac{N}{N_1}\right)\left(\frac{\eta_v}{\eta_{v1}}\right)$$

$$\frac{H}{H_1} = \left(\frac{N}{N_1}\right)^2\left(\frac{\eta_h}{\eta_{h1}}\right)$$

$$\frac{W_{sh}}{W_{sh1}} = \left(\frac{N}{N_1}\right)^3\left(\frac{\eta_{p1}}{\eta_p}\right) \quad .$$

The subscript "1" in the above equations denotes known tests conditions, and η_v, η_h, and η_p are the volumetric, hydraulic, and total pump efficiencies, respectively. Determination of the volumetric and hydraulic efficiencies of the pump are beyond the scope of this program; it will be assumed that the efficiency ratios for the different test conditions are equal to unity, as is often done. The affinity laws may be applied to a test pump to predict parameters different from the known test parameters, or they may be used to normalize pump test data taken at different speeds to one given speed.

The affinity laws were used to normalize the 5000 and 7000 rpm test data to 6000 rpm for comparison to the actual H-Q test data taken at 6000 rpm. The normalized data and the 6000 rpm test data are shown in figure 22; and one can readily conclude that the pump performance data is in excellent agreement with the pump affinity laws for speed variations within this range.

The specific speed is another parameter which is often used to characterize impeller pumps; it also results from the general principles of similitude and is defined as,

$$N_s = \frac{NQ^{1/2}}{H^{3/4}}$$

and is usually computed at the best efficiency point (b.e.p.) of the pump. The best efficiency point of this pump is not precisely defined because of the lack of data points near the peak of the curve, but considering all of the 6000 rpm (design speed) data, the b.e.p. would be near the point indicated in figures 18 and 19. The H-Q values at this point are 9.7 m and 1.6×10^{-4} m^3/s, respectively. Values of N_s are dependent on the units used; in U.S. engineering practice it is customary to use the following units: N(rpm), Q(gal/min), and H(ft). The value for N_s using the customary English units, N = 6000 rpm, Q = 2.54 gal/min, and H = 31.82 ft, is

$$N_s = 712 \qquad \text{(English units)}$$

Centrifugal pumps have values for N_s (English units) in the range of 500 to 3500; thus, this pump is of relatively low specific speed.

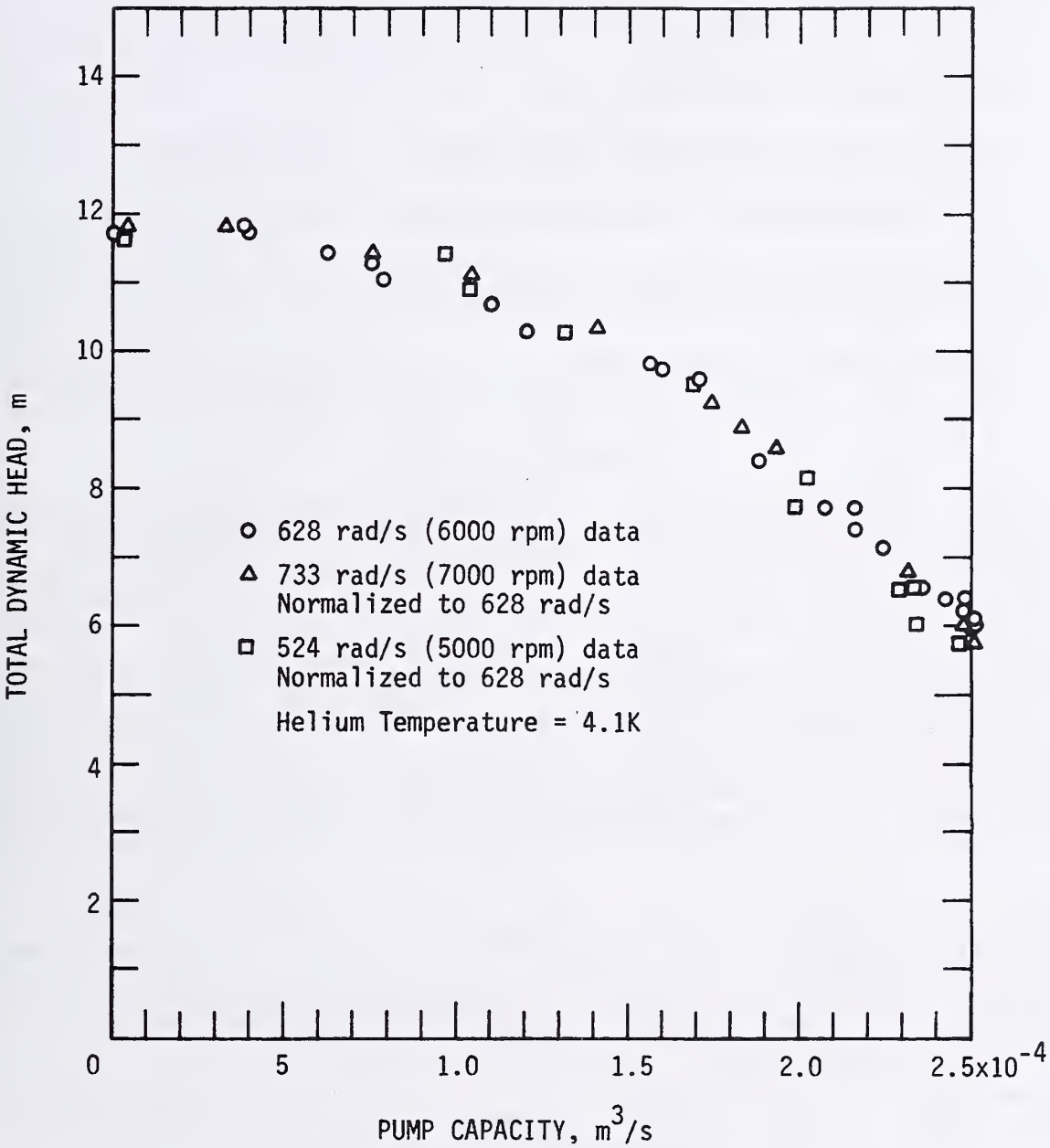

Figure 22. H-Q data normalized to the design speed of 6000 rpm.

Table 1. Liquid helium pump performance data.

Motor Speed	3-phase Frequency	Corrected Power	Pump ΔP $(P_{2g}-P_{1g})$		Venturi ΔP		Mass Flow	Volume Flow	Pressure Head $\left(\frac{P_2-P_1}{\rho g}\right)$	Velocity Head $\left(\frac{V_2^2}{2g}\right)$	Total Dynamic Head	Fluid Power	Total Efficiency	Motor Efficiency
(rpm)	(Hz)	(watts)	(Pa)	(in.H_2O)	(Pa)	(in.H_2O)	(g/s)	(m^3/s)	(cm)	(cm)	(m)	(watts)	(η_t)	(η_m)
5000	360	2.44	10252	41.2	0	0	0	0	806.4	0	8.13	0	0	59
		3.34	9506	38.2	124	0.5	11	0.85×10^{-4}	747.2	3.7	7.58	.82	24.5	62.5
		3.95	8212	33	341	1.37	18.2	1.41×10^{-4}	644.5	10.2	6.62	1.18	29.9	64.2
		4.34	6943	27.9	483	1.94	21.66	1.68×10^{-4}	543.8	14.4	5.65	1.2	27.6	65
		4.72	5524	22.2	647	2.6	25.07	1.95×10^{-4}	431.3	19.4	4.58	1.13	23.8	65.6
		6.5	4753	19.1	722	2.9	26.48	2.05×10^{-4}	370.1	21.5	3.99	1.04	21.2	66
6000	435	3.7	14731	59.2	0	0	0	0	1161.8	0	11.69	0	0	63.2
		5.54	13412	53.9	204	.82	14.08	1.09×10^{-4}	1057.2	6.1	10.7	1.48	26.6	66
		6.64	11870	47.7	485	1.95	21.71	1.69×10^{-4}	934.8	14.6	9.56	2.03	30.6	67.8
		7.4	9456	38	776	3.12	27.47	2.14×10^{-4}	743.2	23.4	7.74	2.08	28.2	69
		7.9	7714	31	995	4	31.1	2.42×10^{-4}	605	29.9	6.42	1.96	24.8	69.8
		8.1	7191	28.9	1058	4.25	32.06	2.49×10^{-4}	563.6	31.7	6.02	1.89	23.3	70
		7.4	9506	38.2	732	2.94	26.66	2.07×10^{-4}	747.2	21.9	7.76	2.03	27.4	69
		5.67	12915	51.9	249	1.0	15.55	1.20×10^{-4}	1016.7	7.4	10.31	1.57	27.7	66.4
		4.75	14159	56.9	67	.27	8.08	0.62×10^{-4}	1116.4	20.3	11.44	0.91	19.1	65
7000	505	5.67	20256	81.4	0	0	0	0	1600.1	0	16.07	0	0	64.1
		7.40	19633	78.9	137	0.55	11.53	0.9×10^{-4}	1550.8	4.1	15.62	1.76	23.8	66.8
		9.25	17618	70.8	460	1.85	21.15	1.64×10^{-4}	1390.8	13.7	14.12	2.93	31.6	69
		10.86	14408	57.9	863	3.47	28.97	2.25×10^{-4}	1136.1	25.9	11.69	11.69	30.6	70.6
		11.74	11173	44.9	1232	4.95	34.6	2.69×10^{-4}	879.5	37	9.24	3.13	26.7	71.4
		12.37	9381	37.7	1468	5.9	37.77	2.93×10^{-4}	737.3	43.9	7.88	2.92	23.6	72
		12.41	9406	37.8	1468	5.9	37.77	2.93×10^{-4}	739.3	43.9	7.9	2.92	23.6	72

A.3. Conclusions From Pump Performance Tests

There are several conclusions resulting from the pump performance tests and the motor efficiency tests. These conclusions are:

1) The use of a submerged cryogenic induction motor to power a simple preinduced, single stage impeller pump is a reliable and efficient method of generating easily controllable liquid helium flow, and

2) the efficiency of this cryogenic motor is dependent upon slip and load, and ranges up to a maximum of 74 percent in liquid helium, and 60 percent in liquid nitrogen,

3) the efficiency of the pump at design speed (6000 rpm) and at the best efficiency point (b.e.p.) is 44 percent,

4) the pump affinity laws are applicable to the non-cavitating H-Q pump performance curves,

5) using a streamline entry, and positioning the impeller for optimum performance, increased the developed head of this pump up to 30 percent at 6000 rpm,

6) plugging the motor coolant passages had no perceivable effect on the H-Q performance of this pump,

7) removing the axial inducer caused a pronounced decrease in the developed head of the pump at flow rates below 1×10^{-4} m^3/s,

8) using reasonable precautions to remove all moisture and condensables by using a thorough helium purge procedure, the pump and motor operation in liquid helium has been routine and trouble-free in our experience.

B. Pump Cavitation Study

In our earlier work [1] some evidence was seen for the beginning of cavitation within the pump when the liquid level dropped to an estimated few centimeters above the pump inlet. The original estimate of the pump designer was that cavitation might develop at liquid levels less than 25 centimeters. The conclusion stated at that time was "a simple inducer-impeller pump can operate satisfactorily in helium I and helium II with little liquid cover. This result may not be universal and needs further testing and evaluation."

An important objective of this work was to explore the cavitation performance of the pump much more carefully, and to correlate it with cavitation performance of other pumps in other cryogenic fluids using some thorough analytical procedures developed within our laboratory [2]. Toward this goal, a broad program was outlined, (a) utilizing improved instrumentation, especially for measuring the helium liquid level, (b) including a wider range of pump speeds, limited in the previous study by the small frequency range of the three-phase power supply, and (c) including a temperature range of about 2.5 to 4.7 K, to test sensitivity of the results to changes in the liquid-to-vapor density ratio.

B.1 Cavitation Test Program

A cavitation test program was outlined that would provide sufficient data such that the computer model capable of predicting cavitation parameters in hydrogen, could be tested to see if the model could be extended to helium. The test program required cavitation data at three different temperatures (2.8, 4.05, and 4.7 K were chosen), at three different pump speeds (4000, 6000, and 7000 rpm), and at three different flow coefficients ($\Phi_1 = 0.1$, $\Phi_2 = 0.16$, and $\Phi_3 = 0.22$ were chosen). Constancy requirements were placed on each of the cavitation parameters in order to satisfy the percent error requirements of the cavitation model. These requirements were:

- Constancy of 1/10% on temperature
- Constancy of 1% of the flow coefficients
- Constancy of 1/2% on the pump speed.

With the test program firmly set, we began to check the operating tolerances necessary to meet the constancy requirements. In order to meet the helium bath temperature requirements, it was necessary to control the ullage pressure within the pressure tolerances listed below:

Temperatures	Pressure Tolerances
2.8 K	± 80 Pa (± 0.6 mm Hg)
4.05 K	± 333 Pa (± 2.5 mm Hg)
4.7 K	± 600 Pa (± 4.5 mm Hg)

It was assumed that the helium bath would be in equilibrium with the ullage pressure of the dewar, and considering the circulation provided by the pump, this appears to be a reasonable assumption. We planned to control the ullage pressure with an NBS barostat which does have the above control capability. Thus the temperature constancy requirements could be met.

The pump speed tolerances are given below; the counts are from the 20 tooth spur gear on the motor shaft.

Pump Speed	Counter Tolerances
4000 rpm	± 7 counts/second
6000 rpm	± 10 counts/second
7000 rpm	± 11 counts/second

During the earlier motor efficiency tests, it was not difficult to maintain a counter tolerance of ± five counts/second; thus the pump speed constancy requirements could be easily met.

The inducer flow coefficient for the cavitation tests is defined as:

$$\Phi = \frac{V_o}{u_t} = \frac{V_o}{2\pi r N}$$

where V_o equals the average flow velocity at the axial inducer inlet, and u_t equals the tip velocity of the inducer. Values of V_o were obtained from the previous H-Q performance data. In order to use the same inducer flow coefficient for all tests, it is necessary to make plots of the flowmeter signal vs the inducer flow coefficient as shown in figure 23. One of these plots is necessary for each temperature. These curves allow one to arbitrarily choose values for each of the three flow coefficients near the low, mid, and high flow ranges, and also to readily determine the flowmeter signal required for tests run at different speeds and temperatures.

The inducer flow coefficient constancy requirement was more severe. In obtaining the H-Q performance data, the mass flow rate was measured with the venturi meter. However, the dial type pressure gauge used to measure the venturi flowmeter ΔP does not have adequate resolution so that one can read pressure differences resulting from one percent variations of the inducer flow coefficient. The minimum discernible value when reading the pressure gauge is 25 Pa (0.1 inches water), and the venturi ΔP pressure excursion for a one percent variation of the flow coefficient Φ_1 at 4000 rpm is ± 0.005 inches of water. Consequently a flow measuring sensor with increased sensitivity was required in order to maintain the inducer flow coefficient values to tolerance of one percent. We decided at this point to place a turbine flowmeter in series with and downstream of the venturi flowmeter in order to obtain a more sensitive flow signal. The flowmeter chosen has an output of 0-600 counts/second for our flow range of 0-38 grams/second. The turbine flowmeter count tolerances for one percent variations of the inducer flow coefficients at 4000 rpm become:

Flow Coefficient (Φ)	Turbine Flowmeter Count Tolerances
Φ = 0.1	± 1.4 counts/second
Φ = 0.16	± 2.3 counts/second
Φ = 0.22	± 3.1 counts/second

When conducting the tests, we found it possible to easily maintain the flowmeter reading to ± 1 count/second. Thus adding the turbine flowmeter provided the increased sensitivity necessary to determine and maintain the flow constancy requirements.

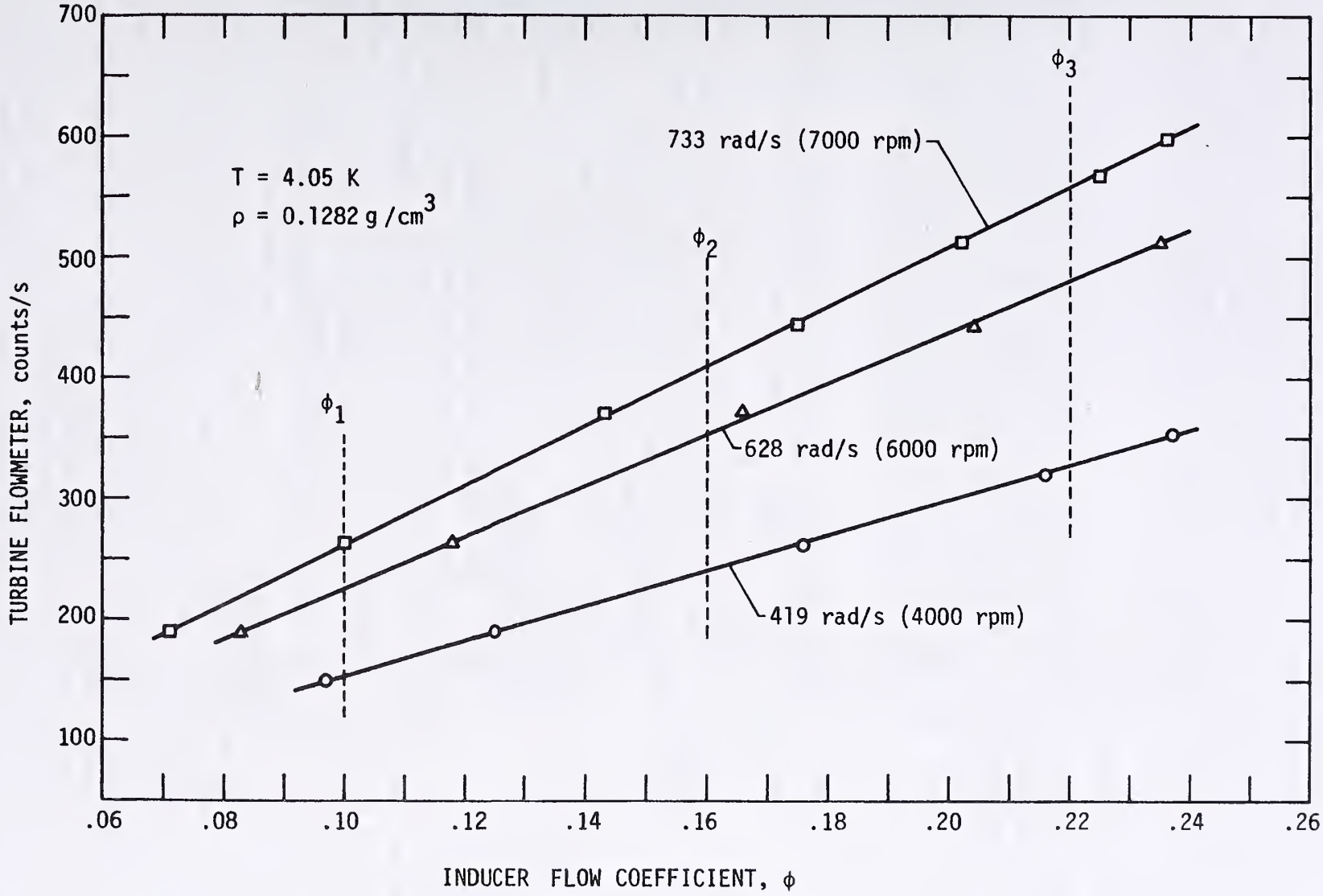

Figure 23. Flow coefficient control data.

At this point we were satisfied that the cavitation parameter constancy requirements could be attained. The other important measurement for cavitation studies is the liquid level. The liquid level sensor used in the previous cavitation tests was a capacitance type, which has marginal sensitivity at liquid helium temperatures. Using a capacitance bridge with a resolution of 0.1 pf, the measurement uncertainty is ± 2 cm in still helium. To improve this, a superconducting liquid level sensor was installed. The sensitivity of the sensor is 326 mV/cm. The liquid level measurement uncertainty is dependent upon calibration procedure, and is estimated to be ± 2 mm in quiescent liquid helium. Having determined the flowmeter signal for the different flow coefficients and being certain the cavitation parameter constancy requirements could be met, we proceeded to run the cavitation tests.

B.2 Cavitation Test Procedure

The cavitation test apparatus is shown in figure 16. The procedure for conducting the cavitation tests was as follows: the dewar would be filled with liquid helium to about 30 cm above the pump inlet (Z_o). The pump would be started, the barostat adjusted to maintain ullage pressure, the discharge valve would be adjusted to attain the flow rate required for the desired Φ, and the pump speed would be attained by varying the voltage to the motor. After adjusting the above test parameters, the pump ΔP, the liquid level, the ullage pressure, the pump speed, the power input, and the turbine meter signal would be periodically recorded as the liquid level decreased due to boil-off. The above parameters would be recorded until the pump ran out of liquid or cavitation occurred.

B.3 Cavitation Test Results

Six different series of cavitation tests were conducted. Five of the series contained cavitation tests run at 4000, 6000, and 7000 rpm, using the three different flow coefficients but all the tests were run at 4.05 K. The last series included cavitation tests with helium at 2.35 K and 4.7 K.

The first series of tests was conducted with the low-entry-loss suction bell and the streamlined inducer nut shown in figure 24. The cavitation data is shown in figures 25 and 26. The numbers on the left side of the data points indicate that several sets of data were recorded while the liquid level sensor was indicating a constant liquid level due to splashing. For cavitation testing, the liquid level measurement is most important because the liquid level is representative of NPSH as explained later in the report. We had difficulties during all the cavitation tests in obtaining an accurate liquid level reading near the main body of the pump. This is undoubtedly due to the discharge helium splashing onto the top of the pump. The superconducting liquid level sensor is composed of a small superconducting wire inside a 8 mm O.D. plastic tube which had 1 mm-diameter holes in line, spaced about 25 mm apart. After the first cavitation test, the holes in the vicinity of the pump base were shrouded to prevent discharge liquid from splashing onto the sensor at this level. The shrouding helped the splashing problem but we still had difficulty in obtaining accurate liquid level readings in the vicinity of the pump, particularly at the higher pump speeds and the high flow rate (Φ_3). Because of the splashing difficulty it was necessary to stop the pump soon after the developed head began to decrease, and obtain an accurate liquid level reading. These liquid level values are indicated on the lower left side in the figures. However, a correction for the liquid in the circulation loop which drains into the bath when the pump is stopped has to be made; this amounts to $\sim$ 35 cm^3 of liquid which increases the helium bath level about 4 mm.

The first series of cavitation tests with the improved instrumentation revealed that instead of cavitating with a positive liquid level, the pump performed very well until it appeared to abruptly cavitate or merely run out of liquid. During a typical test, the pump ΔP, the pump flow rate, and the pump speed would remain constant until the liquid level reached $\sim$ -4 mm, then suddenly the pump ΔP would decrease rapidly and the flow rate would tend to follow. The pump speed would also tend to increase slightly, but this could be easily maintained by adjusting the input voltage. We would try to maintain the constant flow rate (flow coefficient Φ) by opening the flow control valve, but very soon it became impossible to maintain the flow rate and the pump would be stopped. The liquid level after stopping the pump would be near zero. Thus in the first series of tests, the pump did not cavitate with a positive NPSH; the pump either loses suction and begins ingesting vapor or it cavitates abruptly, close to zero NPSH, and in either case precludes the acquisition of any meaningful cavitation data.

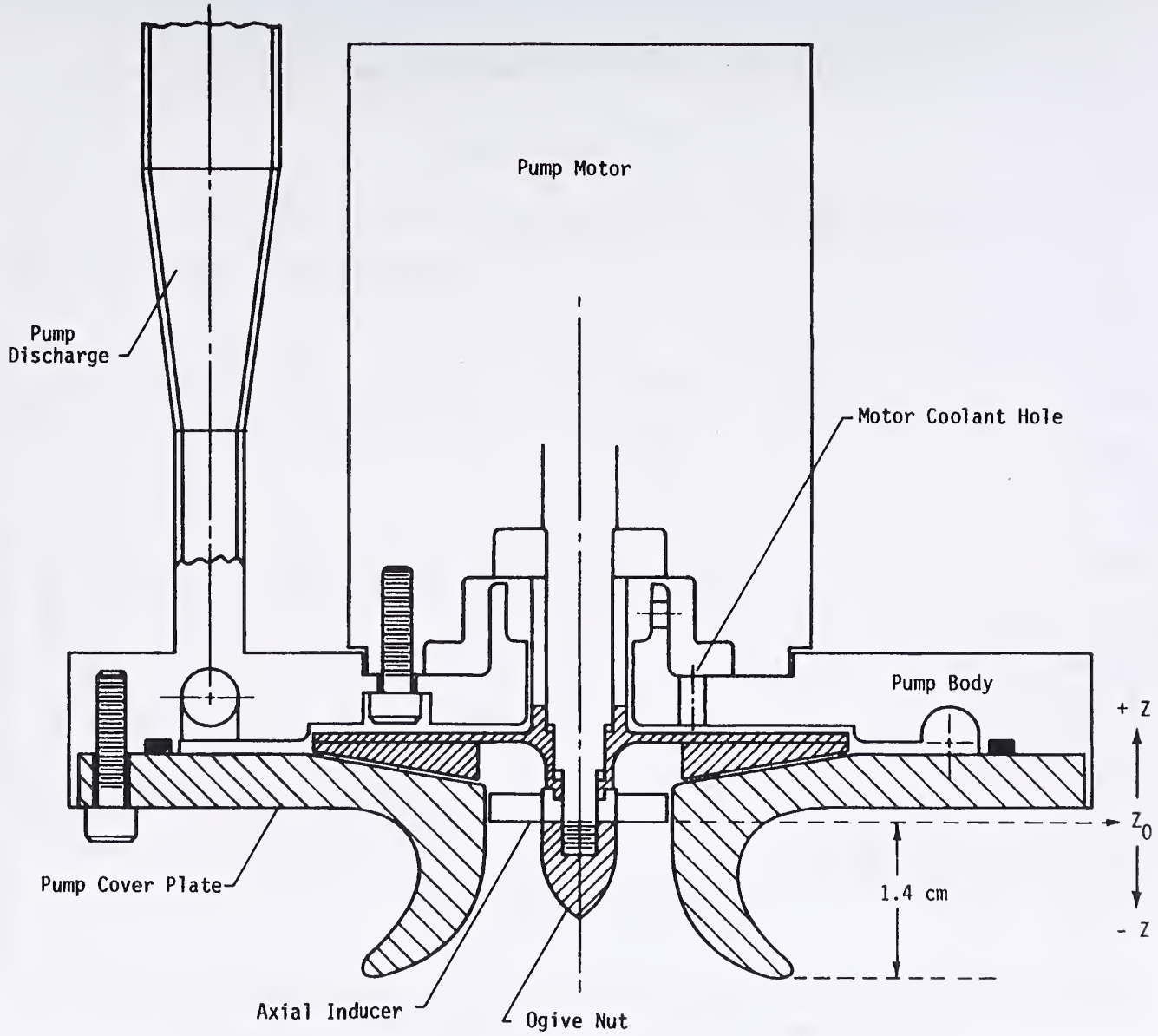

Figure 24. Helium pump with streamline entry.

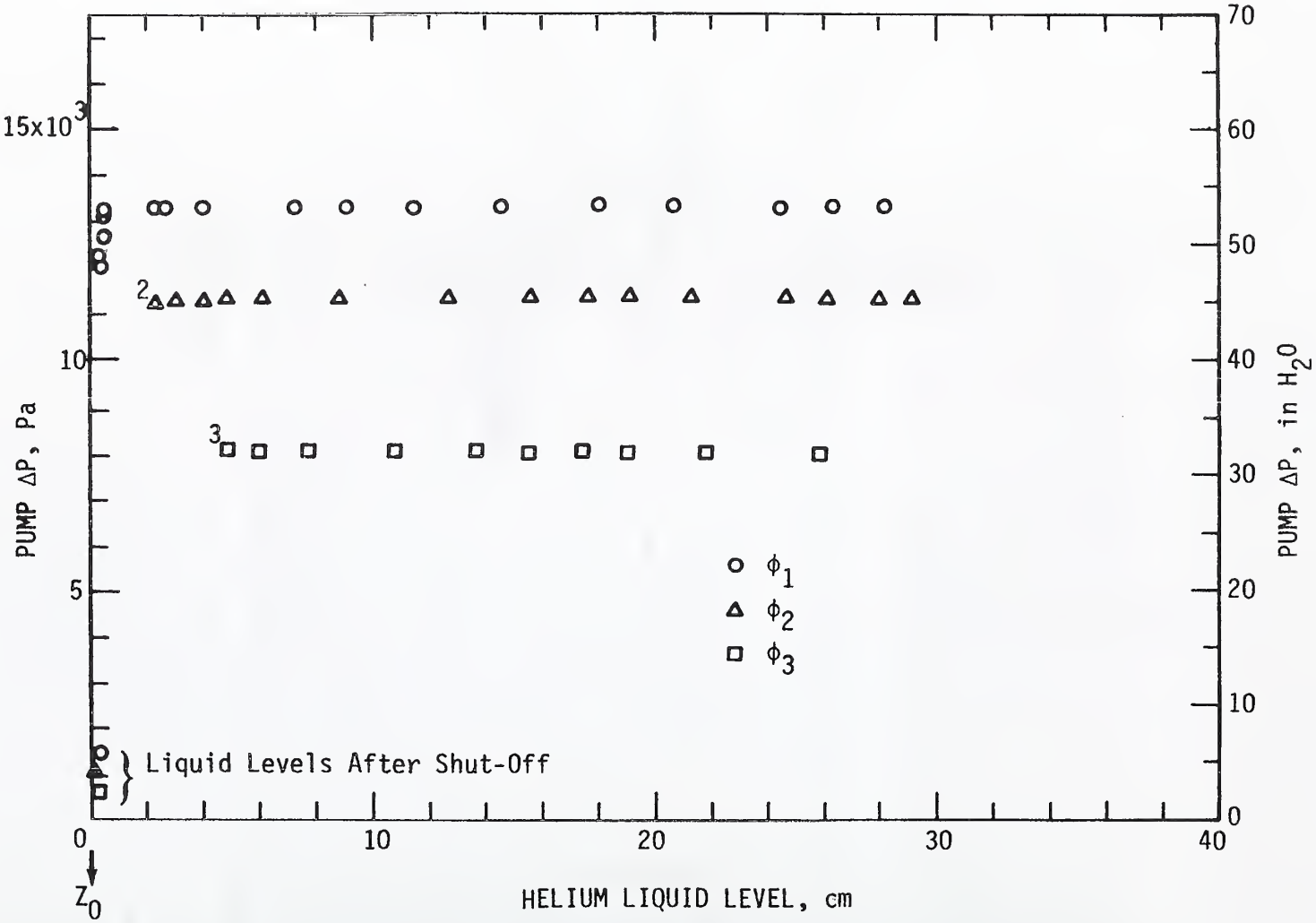

Figure 25. Cavitation data, 6000 rpm, streamline entry.

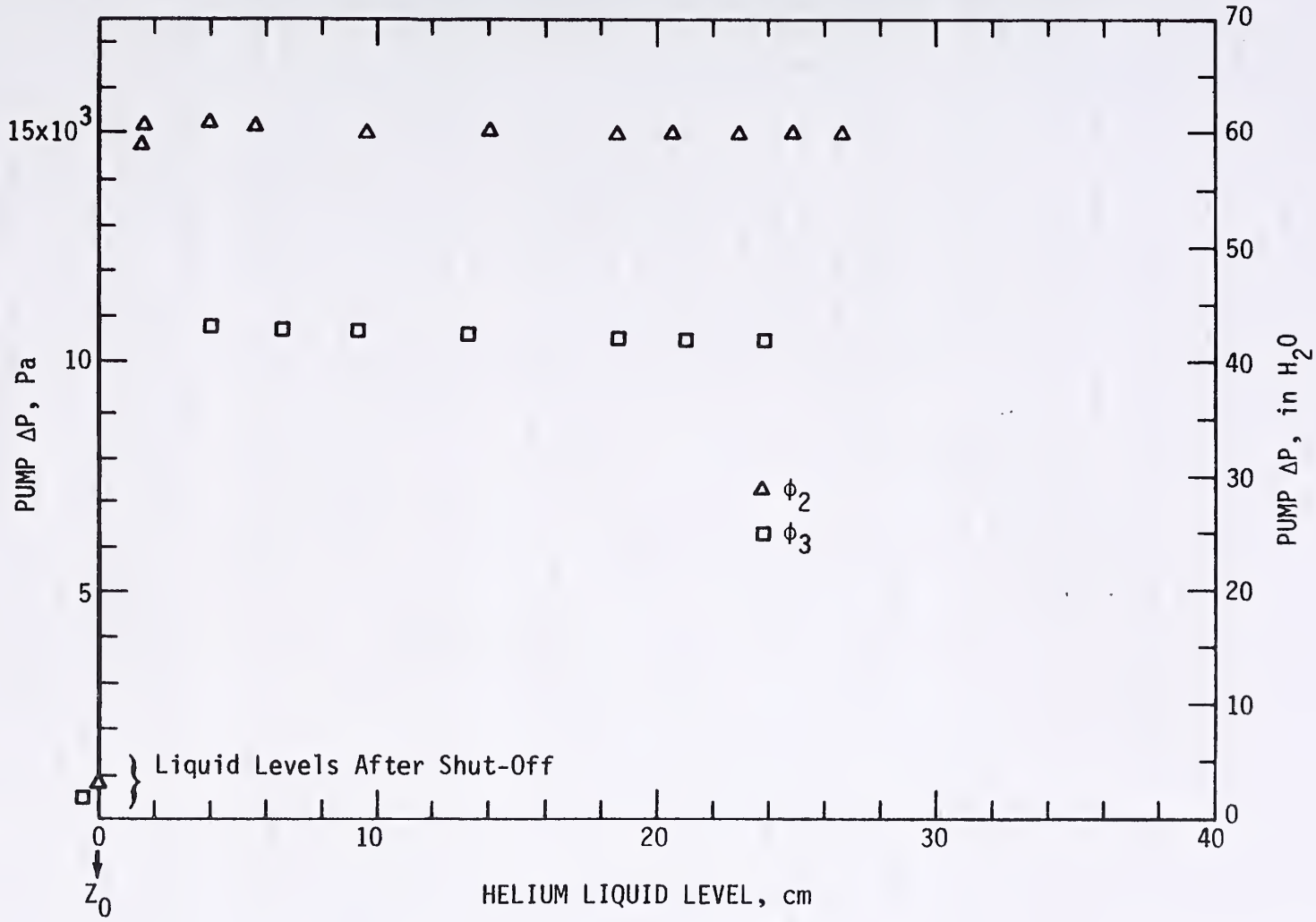

Figure 26. Cavitation data, 7000 rpm, streamline entry.

After failing to observe cavitation in the usual sense, (i.e., a gradual degradation of pump performance at a positive NPSH), we decided to make a number of changes. We lowered the liquid level sensor because the bottom of the sensor extended only slightly below the bottom of the suction bell, giving some concern that we were not getting accurate liquid level measurements in this region. In addition, we decided to shroud the holes in the liquid level sensor near the pump base. We also decided to use a different cover plate for the pump, one having higher entrance losses. The NPSH of a pump operating in a closed vessel pumping a boiling liquid is simply the static liquid level in the vessel above the pump reference plane minus the head losses in the suction pipe (see section B.4). Thus if an entrance tube with high head losses is used on a pump with minimal NPSH requirements, the pump should cavitate at a higher liquid level. The cover plate shown in figure 27 was carefully designed to give a total entry head loss of $1.08\ V_o^2/2g$. However, the entry loss cannot be too high, since we are also concerned about flash vaporization in the pump inlet. If the entry losses are sufficiently high to reduce h_o below h_v, vapor could form upstream of the pump inlet and void the tests. The new cover plate was installed, the liquid level sensor was lowered 7.5 cm and a second series of cavitation tests was run. These cavitation data are shown in figures 28, 29, and 30.

After conducting the first cavitation test (Φ_1), it was quite evident that the helium was still splashing on the liquid level sensor giving us an erroneous reading. Because of this, during the next two tests at Φ_2 and Φ_3, the pump was shut off immediately after a significant decrease in ΔP was noted. The liquid levels were -4.8 cm and -3.8 cm as indicated. The same procedure was used for Φ_1 and Φ_3 in the 6000 rpm tests, and also for the 7000 rpm tests. For the seven tests in this series, all of the liquid level readings at the point where the pump head began to decrease abruptly were in the range of -3 to -5 cm, and it will be shown in section B.4 that the NPSHc ranges from -6.8 to -13.6 cm for this series of tests. There is a possibility that the liquid level reached the bottom of the plate (Z = -7.6 cm) letting the pump ingest vapor and lose suction, but we feel our liquid level uncertainty is ± 2 mm when the motor is off, and that the pump did not lose suction. Thus, once again there is no degradation in pump performance at positive values of NPSH; it appears that the pump cavitates abruptly at negative values of NPSHc, however, there is a remote possibility that it loses suction due to turbulence and splashing in the dewar.

Since the high-entry-loss cover plate didn't have entry losses sufficient to raise the liquid level above the pump when cavitation occurred, and we were reluctant to make them higher because of the likelihood of vapor formation in the inlet, we decided to abandon this inlet geometry and go back to the streamlined cover plate shown in figure 23. We also removed the axial inducer from the pump and used a plain hub in its place. The axial inducer is shown in figure 31 and the hub would merely be an inducer with the blades removed. The pump datum base, which was initially set at the inducer inlet plane (Z_o), was not shifted even though the inducer was removed. All the NPSH and liquid level values in this report are referenced to Z_o as shown in figure 23. The liquid level sensor was not moved.

A third series of cavitation tests was conducted, and once again there was splashing on the liquid level sensor at high speeds and high flow rates. The cavitation data is shown in figure 32. In all the tests, the liquid level after shutting off the pump was about -5 mm, and if one subtracts another 4 mm for the liquid in the circulation loop, it appears as if the pump began to abruptly lose head at a liquid level of -9 mm. However, considering the turbulence in the vessel, there is a good possibility that the pump merely broke suction and started ingesting vapor since the bottom of the suction bell is at a level of -14 mm. Results from this series of tests lead one to the same conclusion; the pump either loses suction and starts ingesting vapor, or it cavitates abruptly at negative values for NPSHc. This series of tests also indicates that the lack of an inducer has no significant effect on the cavitation characteristics of the pump.

We next decided to determine what effect the inducer nut might have on the cavitation characteristics of the pump. To do this a series of cavitation tests were run with a hemispherical nut on the inducer hub, and a second series was run with the original hexagonal

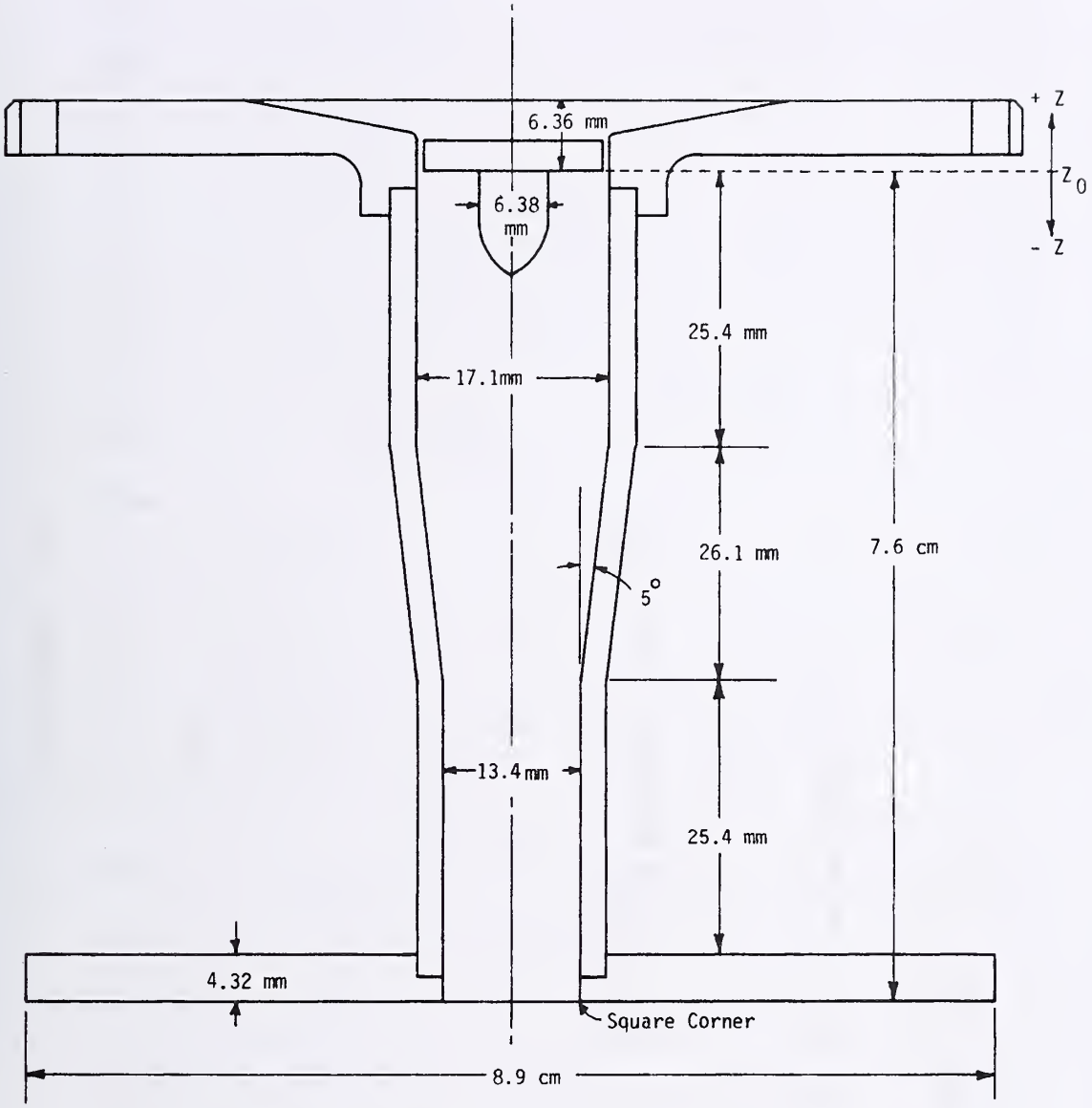

Z_0 is the arbitrary pump datum plane for all cavitation data.

Figure 27. High-entry-loss cover plate.

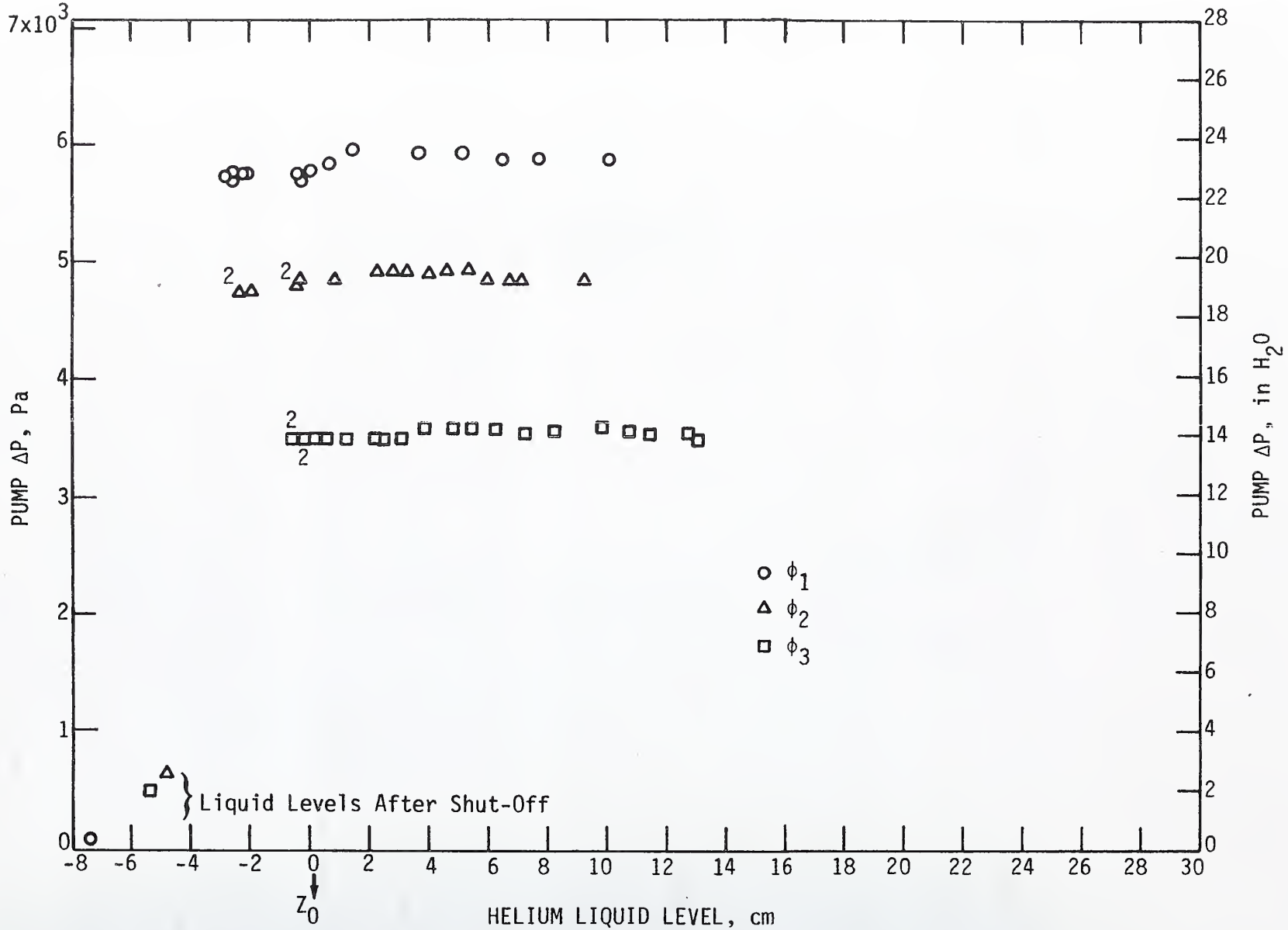

Figure 28. Cavitation data, 4000 rpm, high-entry-loss cover plate.

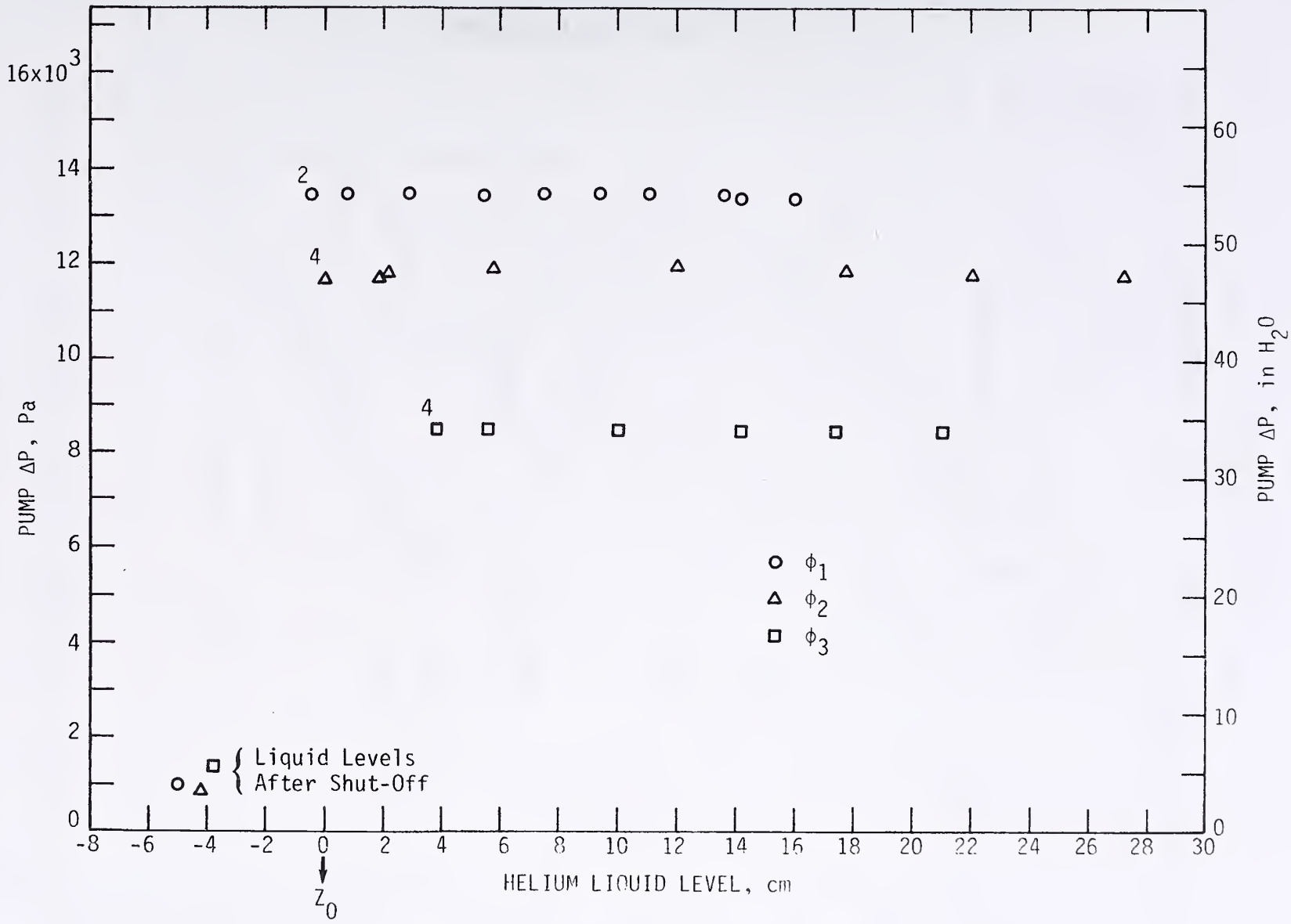

Figure 29. Cavitation data, 6000 rpm, high-entry-loss cover plate.

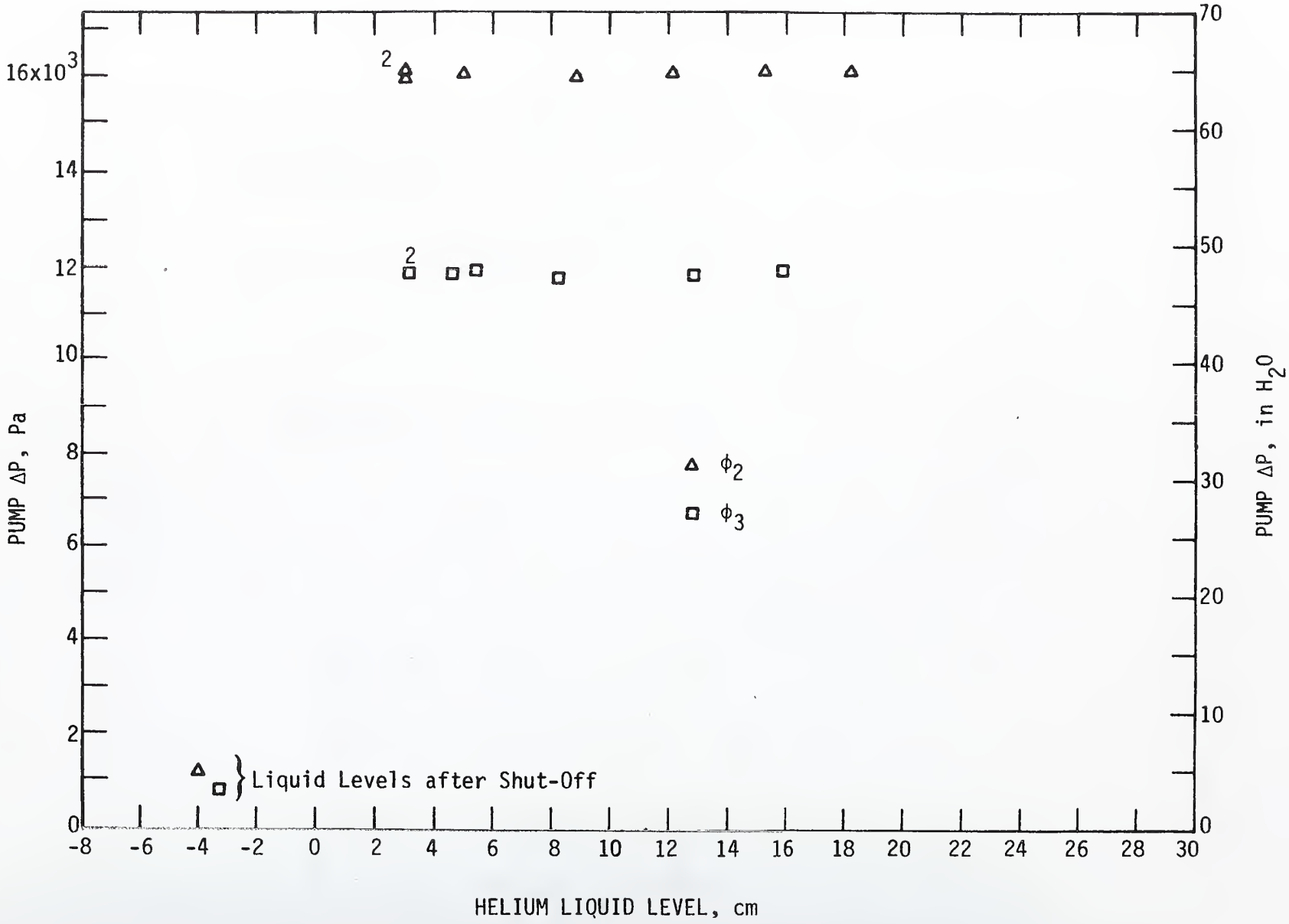

Figure 30. Cavitation data, 7000 rpm, high-entry-loss cover plate.

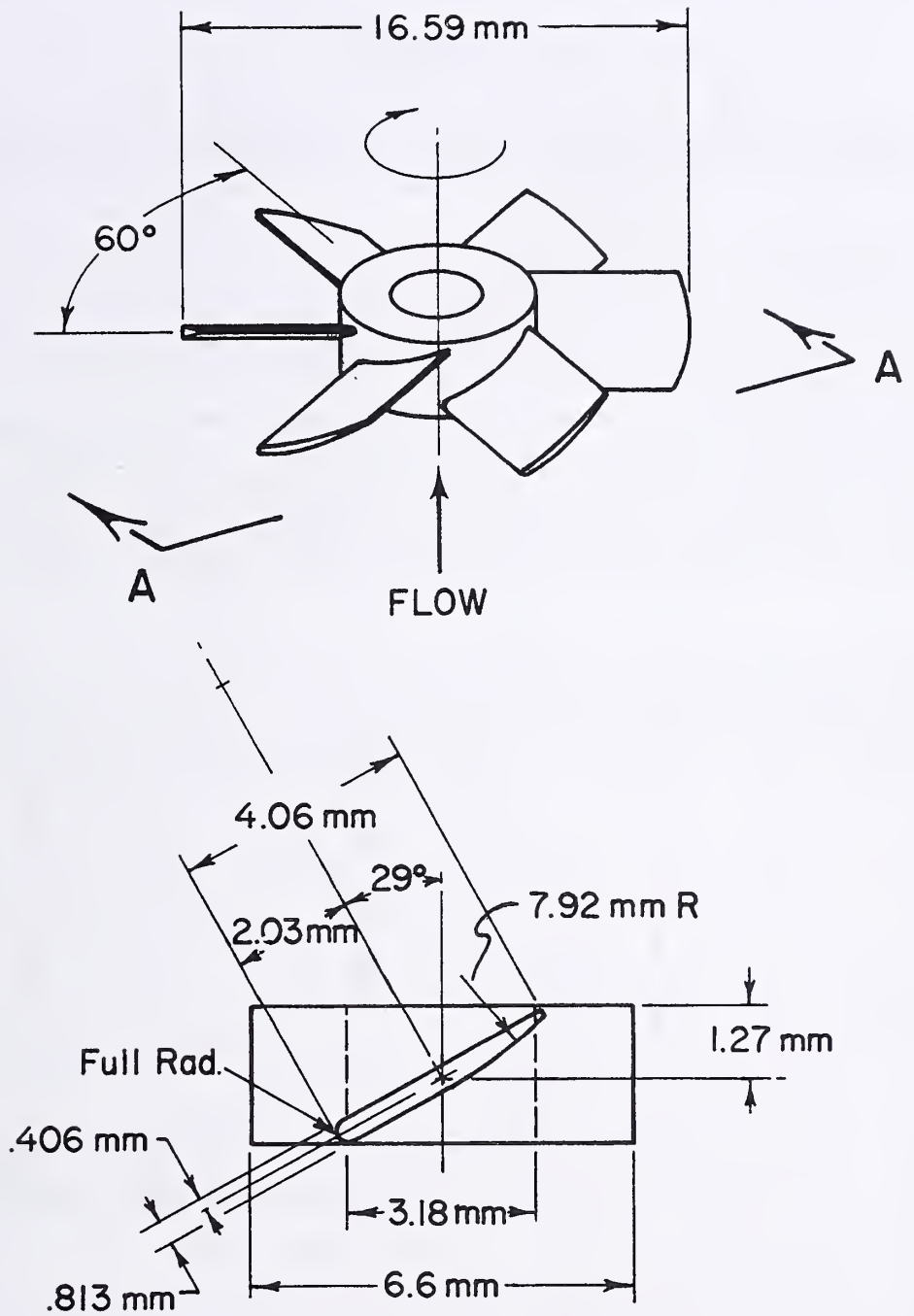

Figure 31. Axial flow inducer.

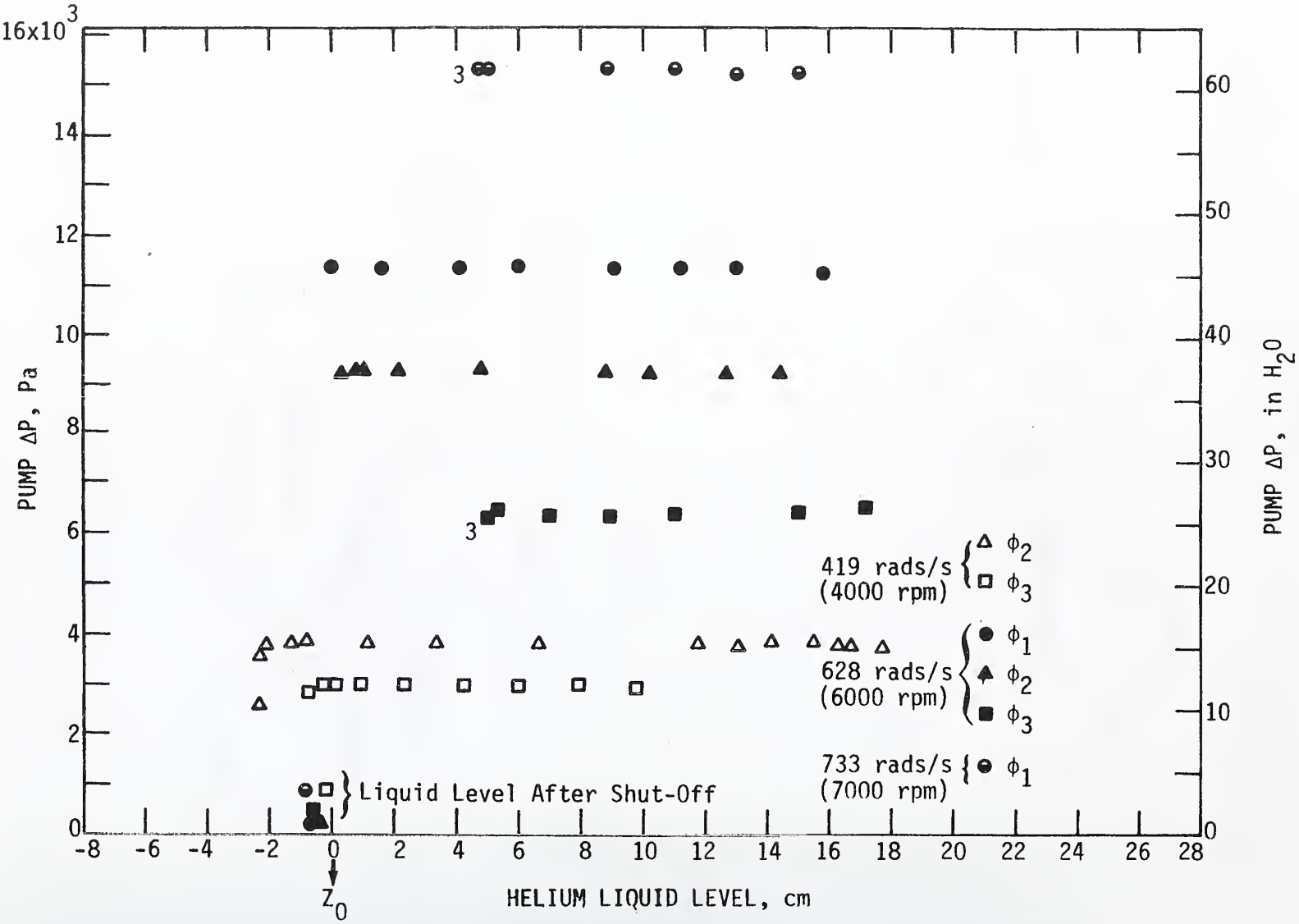

Figure 32. Cavitation data, no inducer, streamline entry.

nut on the inducer hub. Again there was no inducer on the pump for these tests. The results of the two series of tests are plotted together in figure 33. The liquid level after shutting the pump off for most of the tests was about -10 mm, indicating that the pump began to lose developed head when the liquid level was about -14 mm (taking into account the liquid in the pump circulation loop) -- the same level as the bottom of the suction bell. There was no perceivable difference in the developed head or the cavitation characteristics when comparing the two tests using the hemispherical nut and the hexagonal nut; as the plots indicate, the tests are almost a carbon copy of each other. There was no evidence of cavitation within the pump sufficient to affect developed head or flow prior to the liquid level dropping to the same level as the bottom of the suction bell. Data from this series of tests strongly indicate that the pump run out of liquid rather than exhibit any type of cavitation.

Two more cavitation tests were conducted in order to determine if the temperature of the helium had a significant effect on the cavitation characteristics of the pump. Since theory [2] shows that cavitation is strongly dependent on the ratio v_v/v_ℓ or ρ_ℓ/ρ_v, we thought there might possibly be a difference in the cavitation characteristics of helium at 2.35 K and helium at 4.7 K. The value of ρ_ℓ/ρ_v @ 2.35 K = 88.3 and ρ_ℓ/ρ_v @ 4.7 K = 4.17, a significant difference. These comparative tests were run but there was no significant difference in the liquid levels when the pump lost developed head. The test data is shown in figure 34. Once again, the liquid level after shut off averages - 10 mm. Considering the liquid which drains from the circulation loop when the pump is stopped, it again appears as if the pump broke suction and began ingesting vapor when the liquid level reached the bottom of the suction bell. The data also indicates that the temperature of the helium has no effect on the cavitation characteristics of the pump.

B.4 Analysis of the Cavitation Data

For the cavitation tests conducted with the streamlined suction bell, the NPSH is calculated as follows. Using the terminology shown in figure 16, the net positive suction head is defined as the absolute static pressure head at the pump inlet, plus the average velocity head at the pump inlet, less the absolute vapor pressure head at the operating temperature of the liquid at the pump inlet. Thus,

$$NPSH = h_o + \frac{V_o^2}{2g} - h_v, \tag{1}$$

and

$$h_o + \frac{V_o^2}{2g} + h_\ell = LL + h_u$$

and

$$h_o = LL + h_u - \frac{V_o^2}{2g} - h_\ell,$$

so that

$$NPSH = LL + h_u - h_\ell - h_v.$$

Now for an isothermal liquid in equilibrium with its vapor $h_v = h_u$, and

$$NPSH = LL - h_\ell.$$

The long entry tube (figure 27) was designed such that the entry losses are equal to $1.08\ V_o^2/2g$, thus

$$NPSH = LL - 1.08\ \frac{V_o^2}{2g}\ . \tag{2}$$

If the entry losses are assumed negligible, as for the streamlined entry,

$$NPSH = LL. \tag{3}$$

Five different series of cavitation tests were conducted using the streamlined inlet suction bell (figure 24). During these tests the developed head and flow rate began to abruptly decrease when the liquid helium reached the levels indicated below:

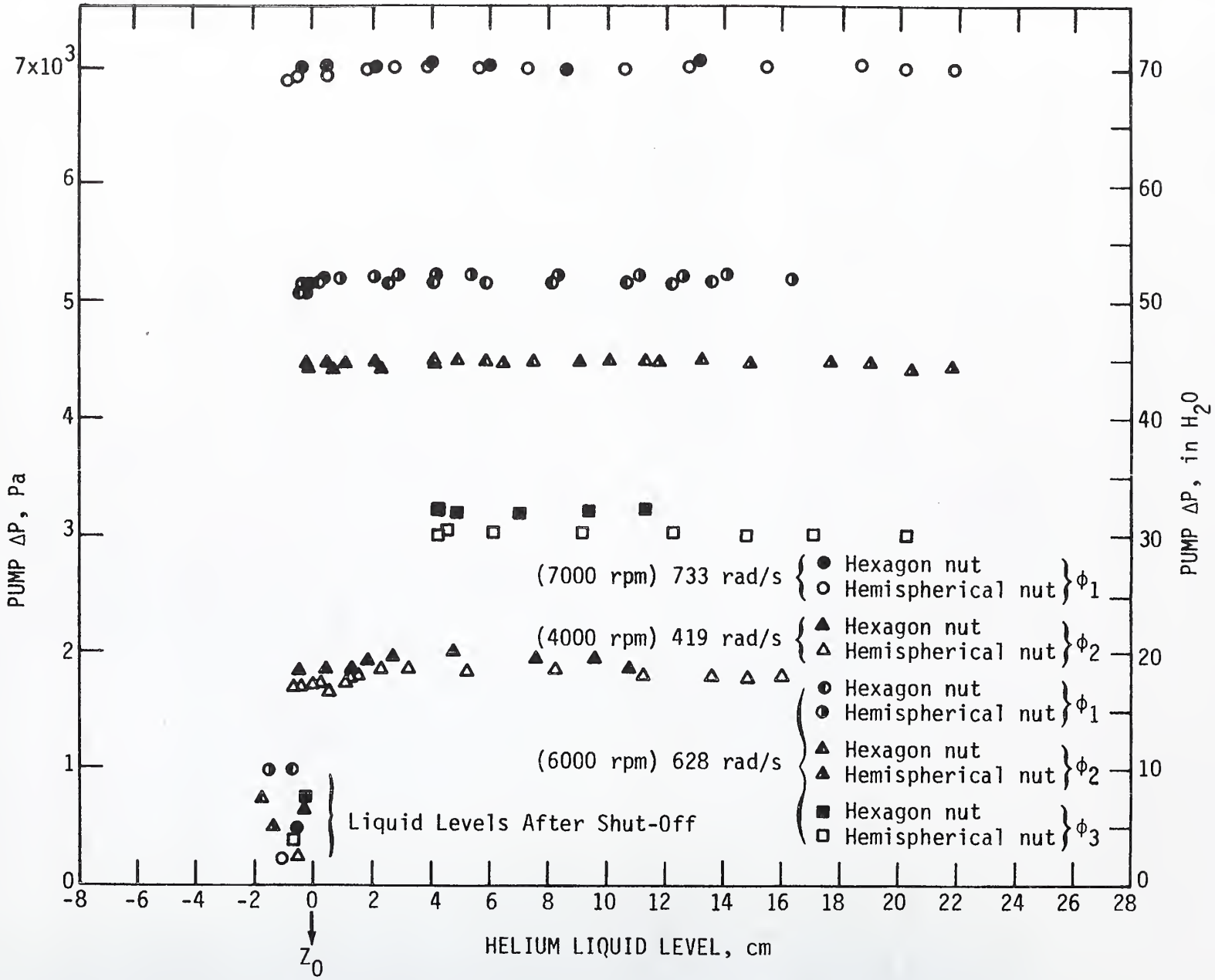

Figure 33. Cavitation data, no inducer, hexagon and hemispherical nuts.

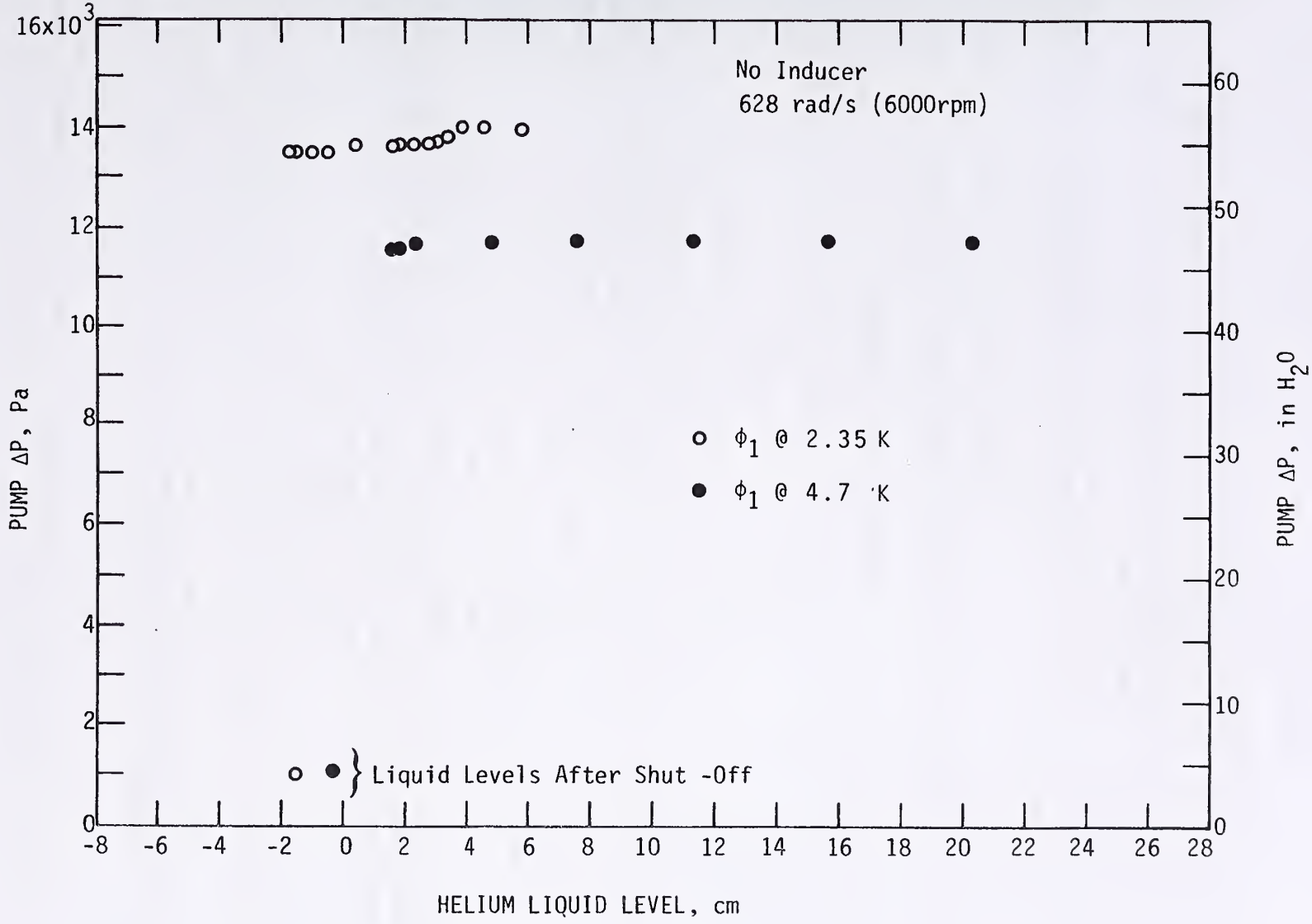

Figure 34. Cavitation data, at temperatures of 2.35 and 4.7 K.

Test series 1	- 1.0 cm
Test series 3	- 1.2 cm
Test series 4 & 5	- 1.4 cm
Test series 6	- 1.3 cm

The above data suggests that the NPSHc for the streamlined entry plate is about - 1.3 cm, the average of the above liquid level values. However, the bottom of the suction bell is at an elevation of - 1.4 cm. Considering the turbulence in the dewar and the uncertainty in the liquid level measurement, it is probably erroneous to speak of the NPSHc, because the data strongly indicates that the pump simply loses suction and starts ingesting vapor when the liquid level reaches the bottom of the suction bell.

Next, calculate the NPSHc for the cavitation tests at 6000 and 7000 rpm with the high-entry-loss cover plate (figure 27). As shown earlier the entry losses have to be considered and they are approximately equal to the velocity head at the pump entry. The magnitude of the term $V_o^2/2g$ is a direct function of the pump speed and the flow coefficient. For our selected conditions, the entry velocity head values are given in the following table.

Table 2. Flow coefficient - entry velocity head values.

	Pump Entry Velocity Head, $V_o^2/2g$ (cm)		
Pump Speed	$\Phi_1 = 0.10$	$\Phi_2 = 0.16$	$\Phi_3 = 0.22$
4000 rpm	0.61	1.57	2.97
6000 rpm	1.38	3.54	6.7
7000 rpm	1.88	4.8	9.1

The NPSHc for the cavitation data taken at 6000 rpm are as follows. During the Φ_1 and Φ_3 flow coefficient tests, the pump was stopped immediately after the head began to decrease, then an accurate liquid level reading was taken. For the test at Φ_1, the liquid level at the start of cavitation was - 5.3 cm. For the test at Φ_3, the liquid level was - 4.2 cm.

The NPSHc calculated using eq. (2) is:

$$\text{for } \Phi_1 \rightarrow \text{NPSHc} = -5.3 \text{ cm} - (1.08 \times 1.38 \text{ cm}) = \underline{-6.8 \text{ cm}}$$

$$\text{for } \Phi_3 \rightarrow \text{NPSHc} = -4.2 \text{ cm} - (1.08 \times 6.7 \text{ cm}) = \underline{-11.4 \text{ cm}}$$

Next consider the cavitation data taken at 7000 rpm. The corresponding liquid levels at the start of pump cavitation are - 4.4 cm and - 3.8 cm, and

$$\text{for } \Phi_2 \rightarrow \text{NPSHc} = \underline{-9.6 \text{ cm}}$$

$$\text{for } \Phi_3 \rightarrow \text{NPSHc} = \underline{-13.6 \text{ cm}}$$

So the NPSHc for the pump using the high-entry-loss cover plate is negative, and in the range of - 6.8 to - 13.6 cm.

The liquid level at which the fluid entering the pump inducer could vaporize and affect the pump performance may also be easily calculated. For the streamlined cover plate, assuming the entry losses are negligible,

$$h_o - h_v = LL - \frac{V_o^2}{2g} \quad .$$

When $h_o - h_v$ is $\leq$ zero, there is a possibility of helium vapor cavities forming at the pump inlet, and the liquid level at which this could start occurring is equal to the inlet velocity head of the pump, i.e., if $h_o - h_v = 0$,

$$LL = \frac{V_o^2}{2g} \quad . \qquad (4)$$

The velocity head for the tests run at 6000 and 7000 rpm ranged from 1.6 to 9.1 cm, but there were no perceivable changes in pump performance when the liquid level was in this range. Thus, if vapor cavities were occurring at the inlet, the cavities were not sufficient to affect the performance of the pump.

Next consider the high-entry-loss cover plate,

$$h_o - h_v = LL - \frac{V_o^2}{2g} + h_\ell$$

or

$$h_o - h_v = LL - 2.08\,\frac{V_o^2}{2g} \quad .$$

Again, when $h_o - h_v \leq$ zero, vapor cavities could form at the inducer inlet. So, there is a possibility of liquid vaporizing at the pump inlet when

$$LL = 2.08\,\frac{V_o^2}{2g} \quad . \tag{5}$$

The cavitation data taken at 6000 rpm with the high-entry-loss cover plate are shown in figure 29. During the Φ_1 and Φ_3 flow coefficient tests, the pump was stopped immediately after the head began to decrease, and an accurate liquid level reading was taken. For the Φ_1 test, the liquid level at the start of cavitation was - 5.3 cm, and for the Φ_3 test, the corresponding liquid level was - 4.2 cm. Now check these liquid levels with the liquid levels required for vapor cavities to occur in the pump inlet:

$$LL_{\Phi_1} = 2.08 \times 1.38 \text{ cm} = \underline{2.87 \text{ cm}}$$

$$LL_{\Phi_3} = 2.08 \times 6.7 \text{ cm} = \underline{13.9 \text{ cm}}$$

Next consider the 7000 rpm data in figure 30. The liquid levels where vapor may begin to form in the inlet are

$$LL_{\Phi_2} = 2.08 \times 4.8 \text{ cm} = \underline{10 \text{ cm}}$$

$$LL_{\Phi_3} = 2.08 \times 9.1 \text{ cm} = \underline{18.9 \text{ cm}}$$

So the liquid levels where vapor cavities could form in the inlet is in the range of 3 to 19 cm for the high-entry-loss cover plate. However, the pump performance at these liquid levels and at lower liquid levels is very steady with very little perturbation in pump head or flow rate. Pump performance is very steady until the liquid level decreases to the - 3 to - 5 cm level, where the pump head and flow rate decrease abruptly.

In comparing the predicted values of liquid level where cavitation should begin with the actual experimental liquid levels where cavitation actually occurred, there is a significant difference. One can only conclude that if vapor cavities are forming at the inlet, they are pumped without impairing the performance of the pump, or the helium passes through the inlet in a metastable state and no vapor cavities occur.

B.5 Conclusions from the Cavitation Tests

Several significant conclusions resulted from the cavitation testing. 1) It was impossible to obtain any meaningful cavitation data from any of our tests which could be used for correlation with liquid hydrogen data in a computer cavitation model. Additional tests were not run at 2.8 and 4.7 K as originally planned because the pump would not cavitate in an acceptable manner. This particular pump shows exceptionally uniform performance over the entire range of positive NPSH values, with no perceivable degradation in developed head, flow rate, or speed until it either fully cavitates in an abrupt fashion (near zero NPSH) or, more likely, just runs out of liquid and starts ingesting vapor. In either case, there is no period during a test wherein there is a gradual degradation of pump performance due to cavitation, during which time conventional cavitation data could be taken.

2) There is no loss in pump performance even when analysis indicates that the static inlet pressure is below the saturated vapor pressure at the operating temperature. This indicates that the helium may be in a metastable state, or slight vapor ingestion may not measurably degrade the pump performance; a possible explanation based upon a few millidegrees of temperature stratification seems not very plausible in this highly turbulent bath. 3) Preliminary cavitation data from the earlier tests [1], conducted with marginal instrumentation for that type of measurement, indicated that cavitation began at an NPSHc of about 9 cm. However, in these tests, with improved instrumentation, no such limit was observed until the liquid level fell below the pump inlet. We suspect that the earlier results were in error, due to an inaccurate liquid level measurement. 4) The temperature of the helium I bath appears to have no appreciable effect on the cavitation characteristics of this pump. 5) The non-cavitating performance of the pump at positive values of NPSH conforms with the conventional affinity laws for centrifugal pumps. 6) Significant inlet geometry changes, including removal of the axial inducer, addition of a turbulence-generating hexagonal nut at the inlet, and addition of a long entry tube providing moderate entry losses, do not cause cavitation in this pump. 7) The pump did not meet the manufacturer's design point specifications, most probably because of an analytical error in the original design. However, it should be stressed that it is possible to accurately design and predict pump performance for a liquid helium pump using conventional pump design parameters and the known thermodynamic properties of helium.

Because of the relatively simple construction of the pump and its freedom from cavitation, even when subjected to the variations described above, we believe that this freedom from cavitation is probably characteristic of the operation of centrifugal pumps in liquid helium.

References

[1] McConnell, P. M., Liquid Helium Pumps, Nat. Bur. Stand. (U.S.) , Interagency Report 73-316 (June 1973).

[2] Hord, J., Cavitation in Liquid Cryogens, Vol. IV, Combined Correlations for Venturi, Hydrofoil, Ogives, and Pumps, NASA CR-2448 (1974).

NoS-114A (REV. 7-73)

U.S. DEPT. OF COMM. BIBLIOGRAPHIC DATA SHEET	1. PUBLICATION OR REPORT NO. NBSIR 75-816 AFAPL-TR-75-40	2. Gov't Accession No.	3. Recipient's Accession No.

4. TITLE AND SUBTITLE
Performance Characteristics of a Liquid Helium Pump

5. Publication Date
June 1975

6. Performing Organization Code

7. AUTHOR(S)
Paul R. Ludtke

8. Performing Organ. Report No.

9. PERFORMING ORGANIZATION NAME AND ADDRESS
NATIONAL BUREAU OF STANDARDS
DEPARTMENT OF COMMERCE
WASHINGTON, D.C. 20234

10. Project/Task/Work Unit No.
2750154

11. Contract/Grant No.

12. Sponsoring Organization Name and Complete Address (*Street, City, State, ZIP*)
Part (A) Wright-Patterson Air Force Base
Dayton, Ohio 45433
Part (B) Defense Advanced Research Projects Agency
1400 Wilson Blvd., Arlington, Virginia 22209

13. Type of Report & Period Covered
Final

14. Sponsoring Agency Code

15. SUPPLEMENTARY NOTES

16. ABSTRACT (*A 200-word or less factual summary of most significant information. If document includes a significant bibliography or literature survey, mention it here.*)

Part A of this report presents performance data for a simple, preinduced, single stage, centrifugal liquid helium pump powered by a close-coupled submersible cryogenic induction motor. Data on pump efficiency and the motor efficiency are given, and the effects of decreasing the pump leakage loss and removing the pre-inducer were also investigated.

Part B describes a study of the cavitation characteristics of the pump in liquid helium I. The net positive suction head at cavitation of the pump was extensively investigated, and found to be near zero; the effects of removing the inducer, changing the pump inlet geometry, and varying the helium temperature were determined.

17. KEY WORDS (*six to twelve entries; alphabetical order; capitalize only the first letter of the first key word unless a proper name; separated by semicolons*)
Cavitation; cryogenic motors; induction motors; liquid helium pumps; motor efficiency; net positive suction head; pump efficiency; pump performance.

18. AVAILABILITY
[X] Unlimited
[ ] For Official Distribution. Do Not Release to NTIS
[ ] Order From Sup. of Doc., U.S. Government Printing Office Washington, D.C. 20402, SD Cat. No. C13
[X] Order From National Technical Information Service (NTIS) Springfield, Virginia 22151

19. SECURITY CLASS (THIS REPORT)
UNCLASSIFIED

21. NO. OF PAGES
55

20. SECURITY CLASS (THIS PAGE)
UNCLASSIFIED

22. Price
$4.25

USCOMM - ERL 2-P74